MASS TRANSFER AROUND SINGLE SPHERES IN THE PRESENCE OF LARGE TEMPERATURE GRADIENTS

MASS TRANSFER AROUND SINGLE SPHERES IN THE PRESENCE OF LARGE TEMPERATURE GRADIENTS

by

RONALD R. ADAMS

A Thesis

Submitted to the Faculty of Graduate Studies

in Partial Fulfilment of the Requirements

for the Degree

Master of Science

McMaster University

June 1968

MASTER OF SCIENCE (1968)
(Metallurgy)

McMASTER UNIVERSITY
Hamilton, Ontario

TITLE: Mass Transfer Around Single Spheres in the Presence of Large Temperature Gradients.

AUTHOR: Ronald R. Adams, B.Sc. (McMaster University)

SUPERVISORS: Professors W.-K. Lu and A. E. Hamielec

NUMBER OF PAGES: (viii); 79

SCOPE AND CONTENTS:

Forced convection mass transfer rates to single spheres with fast surface reaction were calculated in the presence of large temperature gradients. The energy and continuity equations were solved by a finite difference method and the results correlated with film temperature approximations. A correction factor was developed which allows calculation of the fluxes from the film temperature approximations.

ACKNOWLEDGEMENTS

The author is grateful to Drs. W.-K. Lu and A. E. Hamielec for guidance and encouragement throughout this study.

The financial assistance of Dominion Foundries and Steel Limited is gratefully acknowledged.

NOMENCLATURE

A_1, A_2, A_3, A_4 B_1, B_2, B_3, B_4	constants in velocity profiles
A, B	arbitrary constants in empirical equation (R-3)
a, b	constants in molecular diffusivity
C	concentration, moles/cm^3
C_p	constant pressure heat capacity, cal/mol/deg.
D_{AB}	molecular diffusivity in binary gas mixture at low pressure, cm^2/sec.
D_p	sphere diameter, cm.
Gr	Grashof number ($= \frac{8R^3 \rho^2 g \beta \Delta T}{\mu^2}$)
i. j	positions in finite difference mesh
K	thermal conductivity, cal/cm/sec/^oK
K_H	heat transfer coefficient, cal/cm^2/sec/^oK
K_m	mass transfer coefficient, moles/cm^2/sec
M	molecular weight
N_{Nu}	Nusselt number ($= \frac{2.R.K_H}{K}$)
N_{Sh}	Sherwood number ($= \frac{2.R.K_M}{C.D_{AB}}$)
Pe_H, Pe_M	Peclet numbers for heat and mass transfer ($Pe_H = \frac{2RU}{\alpha}$ $Pe_M = \frac{2R.U}{D_{AB}}$)
p_c	critical pressure of a gas, atm.
r	any radial distance from sphere
R	sphere radius, cm.

Re	Reynolds number (= $\frac{2R.U.\rho}{\mu}$)
T	temperature, ^{o}K
T_c	critical temperature of a gas, ^{o}K
U	bulk fluid velocity, cm/sec
V	velocity component, cm/sec
X	ratio of drop temperature to bulk temperature
Y	mole fraction
α	thermal diffusivity (= $\frac{K}{\rho.Cp}$), $cm^2/sec.$
β	volume coefficient of expansion ($^{o}K^{-1}$)
ρ	density, g/cm^3
Φ	weight factor in thermal conductivity
μ	viscosity, poise
ν	kinematic viscosity (μ/ρ) cm^2/sec
Θ	angle, radius
σ	- Lennard-Jones parameter in viscosity calculation, $\mathring{A}$ - standard error of estimate
$\Omega\mu$	parameter in viscosity calculation

Subscripts

A	first gas in binary mixture
B	second gas in binary mixture
i, j	coordinates of finite difference mesh points
s	surface
Θ	in an angular direction
∞	in the bulk gas

Superscripts

*	indicates a dimensionless quantity

TABLE OF CONTENTS

LIST OF TABLES

LIST OF ILLUSTRATIONS *

---

* Illustrations have been placed at the end of the thesis.

CHAPTER 1

INTRODUCTION

Operations involving mass transfer to or from spherical particles of gas, liquid, or solid are becoming of increasing concern to the steel industry. In this category are: the growth of solid inclusions in a liquid melt, CO pickup by gas bubbles in bottom-blown processes, absorption of gases and oxidation of splashing metal during pouring and teeming operations, and the refining of carbon-rich pig iron droplets by reaction with an oxygen-rich atmosphere in the "spray refining" process (1,2,6,8).

The effect of steep temperature gradients on rates of mass transfer in the gas phase around droplets of hot metal were investigated theoretically over a wide range of temperatures and gas compositions.

This work is largely an extension to non-isothermal systems of solutions developed by Houghton (13) for mass transfer with chemical reaction around spheres.

The accuracy of a theoretical prediction of mass transfer to or from spheres in a fluid stream depends greatly on the accuracy of the local velocity distribution around the sphere. Many local velocity distributions exist, each valid over different ranges of Reynolds numbers. In the range $1 \leq Re \leq 500$ (of interest in this study) Houghton (13) found the most accurate descriptions to be those of Hamielec et al (10,12).

In studies of small spheres moving in a fluid medium Reynolds numbers are less than 200. The local velocity profiles of Hamielec et al.

(10,12) have therefore been used in the present theoretical analysis of forced convection mass transfer in the gas phase.

To simplify the solutions, certain assumptions (which will be elaborated upon later) were made. For instance, in the heat transfer calculations radiation was neglected, but it could easily be added, as shown in the Appendix. Thermal diffusion was neglected from the mass flux calculations to simplify the equation of continuity. Rough estimates of thermal diffusion were made (5, pg. 575) justifying this assumption.

The strategy adopted in the present study will become clear with the following considerations: it is standard practice (5,9,11,13) to calculate heat and mass fluxes using isothermal equations based on the use of an effective temperature (referred to as film temperature), that temperature being an arithmetic mean of the drop and bulk temperatures. There is no theoretical justification in the literature for the empirical approach of accounting for steep temperature gradients. The present investigation aims to provide some theoretical justification or to establish a more accurate empirical procedure.

CHAPTER 2

THEORETICAL CONSIDERATIONS

The purpose of this study is to calculate the mass flux of oxidizing gas from a flowing binary mixture at low temperature to a sphere at high temperature with which the gas reacts. Because of the non-isothermal nature of the problem, the energy equation is first solved (in the form of Equation (T-4) shown later) to give the temperature profile around the sphere and then these temperatures are used to modify the physical parameters in the continuity equation (Equation (T-3)) which, when solved, gives concentration profiles of oxidizing gas around the sphere and also the mass flux to the sphere surface.

A. Convection Equation

i) Mass Transfer

By making a mass balance on the volume element shown in Figure (A-1) (as in Appendix A) the following convection equation can be developed with the use of the equation of continuity:

$$V_r \frac{\partial c}{\partial r} + \frac{V\Theta}{r} \frac{\partial c}{\partial \Theta} = D_{AB} \left(\frac{\partial^2 c}{\partial r^2} + \frac{2}{r} \frac{\partial c}{\partial r} + \frac{\cot\Theta}{r^2} \frac{\partial c}{\partial \Theta} + \frac{1}{r^2} \frac{\partial^2 c}{\partial \Theta^2}\right) \qquad (T\text{-}1)$$

assuming D_{AB} is constant*.

---

* See Appendix B for details

The boundary conditions to be satisfied for the physical situation previously described follow:

$c = c\ (bulk)$ as $r \to \infty$

$c = 0$ as $r \to R$

$\frac{\partial c}{\partial \Theta} = 0$ at $\Theta = 0, \pi$ (as a result of axial symmetry)

To reduce the number of physical parameters equation (T-1) was made dimensionless in the following manner:

$$V_r^* = \frac{V_r}{U} \qquad V^* = \frac{V_\Theta}{U}$$

$$r^* = \frac{r}{R} \qquad c^* = \frac{c - C_s}{c(bulk) - C_s}$$

$$Pe_M = \frac{D_p . U}{D_{AB}}$$

giving equation (T-2) (the asterisks are dropped):

$$V_r \frac{\partial c}{\partial r} + \frac{V_\Theta}{r} \frac{\partial c}{\partial \Theta} = \frac{2}{Pe_M} \left[\frac{\partial^2 c}{\partial r^2} + \frac{2}{r} \frac{\partial c}{\partial r} + \frac{\cot\Theta}{r^2} \frac{\partial c}{\partial \Theta} + \frac{1}{r^2} \frac{\partial^2 c}{\partial \Theta^2}\right] \qquad (T\text{-}2)$$

Johnson and Akehata (15) and Houghton (13) both cited difficulties in solving equation (T-2) for Pe > 100. In order to make computation times and computer storage requirements reasonable, Houghton reduced equation (T-2) (which is elliptic in both radius and angle) to a form which was parabolic in angle but still elliptic in radius. This was accomplished by assuming that molecular diffusion in the angular direction was much smaller than that in the radial direction, making it

possible to drop out terms in $\frac{\partial c}{\partial \Theta}$, $\frac{\partial^2 c}{\partial \Theta^2}$ on the right-hand side:

$$V_r \frac{\partial c}{\partial r} + \frac{V_\Theta}{r} \frac{\partial c}{\partial \Theta} = \frac{2}{Pe_M} \left[\frac{\partial^2 c}{\partial r^2} + \frac{2}{r} \frac{\partial c}{\partial r} \right] \qquad (T\text{-}3)$$

Equation (T-3) is valid at a fixed point in space for steady-state, axisymmetric, incompressible flow. In this non-isothermal system Pe_M is a function of position around the sphere, and the manner in which this variation was accounted for will be elaborated in a later section.

Regarding the assumptions made in developing the convection equation: steady state, incompressible, axi-symmetric flow with constant diffusivities (D_{AB} and α). The last has been dealt with in Appendix B. Steady state conditions are never quite realized in a falling drop, especially if it is accelerating. It is, however, very much simpler to divide the distance fallen into a series of pseudo-steady state zones and calculate each one separately (by calculating Re as a function of time) than it is to leave the equation as a differential equation in time. Because all the properties of the system should be smoothly continuous in time (provided a small enough zone size is chosen) there should be no problems encountered as a result of this.

The simplifying assumption of axial symmetry is justified for small droplets with large surface tension forces.

The incompressibility of the flow in an isothermal system would be justified on the basis of the low Reynolds numbers ($10 \leq Re \leq 100$) used in the calculations. This same justification will be used here as

far as the equation of continuity is concerned so that the fluid mechanics of isothermal systems may be used. It must be pointed out, however, that the density is actually allowed to change in the flux calculations.

This inconsistency is again a result of the attempts to make the mathematics tractable, but it is not an original assumption. Theoretical natural convection studies in the past (3) have assumed properties to be constant in the solution of the momentum equation that they allowed to vary in other parts of the solution (for example, in the calculation of gravitational body forces due to buoyancy in the gas stream).

Resistance to mass transfer at the sphere surface is assumed to be zero (surface reaction is relatively very fast) and any products formed have no effect on transport in the system.

ii) Heat Transfer

The study of forced convection heat transfer around a sphere in a flowing gas stream as described earlier leads to an equation analagous to equation (T-3); namely:

$$V_r \frac{\partial T}{\partial r} + \frac{V_\Theta}{r} \frac{\partial T}{\partial \Theta} = \frac{2}{Pe_H} \left[\frac{\partial^2 T}{\partial r^2} + \frac{1}{r} \frac{\partial T}{\partial r}\right] \qquad (T\text{-}4)$$

where $T(\text{dimensionless}) = \dfrac{T - T_\infty}{T_d - T_\infty}$

$$Pe_H = \frac{D_p . U}{\alpha} \qquad \alpha = \frac{K}{\rho . C_p}$$

Natural convection is neglected with respect to forced convection because of the very small value of (Gr/Re^2) (5, pg. 413).

iii) Velocity Profiles

In order to solve the mass transfer and heat transfer equations (T-3) and (T-4) it is necessary to have a description of the velocity profiles around the sphere under study as a function of position. The profiles used were those developed by Hamielec et al. (10,12).

The velocity profiles used may be written as functions of r and Θ in the following way:

$$V_r = \left[-1 + \frac{2A_1}{r^3} + \frac{2A_2}{r^4} + \frac{2A_3}{r^5} + \frac{2A_4}{r^6}\right] \cos\Theta$$

$$- \left[\frac{B_1}{r^3} + \frac{B_2}{r^4} + \frac{B_3}{r^5} + \frac{B_4}{r^6}\right] (2\cos^2\Theta - \sin^2\Theta)$$

$$V_\Theta = \left[-1 - \frac{A_1}{r^3} - \frac{2A_2}{r^4} - \frac{3A_3}{r^5} - \frac{4A_4}{r^6}\right] \sin\Theta$$

$$- \left[\frac{B_1}{r^3} + \frac{2B_2}{r^4} + \frac{3B_3}{r^5} + \frac{4B_4}{r^6}\right] \sin\Theta\cos\Theta$$

where, for a solid or non-circulating sphere:

$$A_2 = \frac{-(120 + 75A_1)}{29} \qquad B_2 = \frac{-69B_1}{27}$$

$$A_3 = \frac{(153 + 63A_1)}{29} \qquad B_3 = \frac{57B_1}{27}$$

$$A_4 = \frac{-(47.5 + 17A_1)}{29} \qquad B_4 = \frac{-15B_1}{27}$$

Values of A_1 and B_1 have been tabulated for several values of Re (12) and non-linear interpolation between these values quite simply produces intermediate values (see Appendix C). These velocity fields are based on a solution for isothermal flow of a Newtonian fluid.

Because of the presence of large temperature gradients, some question might arise as to the best value of temperature at which to evaluate the Reynolds number. Since the Reynolds number calculation is separate from this, it is suggested that it be evaluated at the drop temperature.

No compensation was made for the deformation of the drop from a spherical shape. The high surface tension of liquid iron made the assumption valid for the systems of concern here, but if the calculations were to be applied to other systems this point should be kept in mind.

The same is true of the assumption that the drop was not circulating internally at any time. Because experimental work to correlate with this study would use wire-melting techniques (4) to produce stagnant (interior not in motion) falling drops, the "rigid sphere" concept was considered acceptable. The inertia of the drop, when compared to the drag on its surface as it falls, was just too great for the short times (less than 1 sec.) of fall to make the start of stirring significant. It would be fairly straightforward to allow circulation of the drop; it involves a more general form of the velocity profiles in the numerical solutions.

B. Temperature-Dependent Parameters in Binary Gas Mixtures

The continuity and energy equations contain two parameters which were considered to be functions of temperature, namely, Pe_M and Pe_H.

$$Pe_M = \frac{D_p . U}{D_{AB}} \qquad Pe_H = \frac{D_p . U}{\alpha} \qquad \text{where } \alpha = \frac{k}{\rho . C_p}$$

This requires the knowledge of the terms making up Pe_M and Pe_H as functions of temperature. The forms used were the following:

i) Molecular diffusivity (5):

$$D_{AB} = a.(p_{C_A} . p_{C_B})^{1/3} \left(\frac{1}{M_A} + \frac{1}{M_B}\right)^{1/2} T^b . (T_{C_A} . T_{C_B})^{\left(\frac{5}{12} - \frac{b}{2}\right)}$$

where for pressures of the order 1 atm.

$$a = 2.745 \times 10^{-4} \qquad b = 1.823$$

for non-polar gas pairs (eg. N_2 - O_2)

ii) Thermal conductivity:

$$K = \frac{X_A \cdot K_A}{X_A \phi_{AA} + X_B \phi_{AB}} + \frac{X_B K_B}{X_A \phi_{BA} + X_B \phi_{BB}}$$

where $$\phi_{i,j} = \frac{1}{\sqrt{8}} \left[1 + \frac{M_i}{M_j}\right]^{-1/2} \left[1 + \left(\frac{\mu_i}{\mu_j}\right)^{1/2} \left(\frac{M_j}{M_i}\right)^{1/2}\right]^2$$

and $$\mu_A = 2.6693 \times 10^{-5} \frac{(M_A . T)^{1/2}}{(\sigma^2 \, \Omega_\mu)}$$

iii) Density:

Ideality was assumed to calculate density from

$$\rho = \frac{P}{RT}$$

iv) Heat capacity (C_p):

Expressing the molar heat capacity as a power series in T (17):

$$C_p = C_p(0) + C_p(1)T + C_p(2)T^2$$

the heat capacity can be calculated as a function of temperature for any gas from tabulated values of $C_p(0)$, $C_p(1)$, $C_p(2)$.

The heat capacity of a binary mixture was calculated from:

$$C_p = Y_A . C_{pA} + Y_B . C_{pB}$$

C. Solution of the Transport Equations

Solutions to the mass transfer and heat transfer equations (T-3) and (T-4) are required at each point in space. From these solutions mass transfer and heat transfer rates can be calculated from the gradients at the surface of the sphere.

$$N_{Sh} = \frac{D_p . k_M}{D_{AB}} = - 2. \left.\frac{\partial c^*}{\partial r^*}\right| r^* = 1$$

$$\text{flux} = - D_{AB} . \frac{\partial c}{\partial r} = K_M \, (C(\text{bulk}) - C_s)$$

and similarly for heat transfer

$$N_{Nu} = \frac{D_p . k_H}{K} = - 2. \left.\frac{\partial T^*}{\partial r^*}\right| r^* = 1$$

From these the average transfer rate over the surface of the sphere up to the flow separation angle is:

$$\overline{N_{Sh}} = \int_0^{\Theta_s} \frac{N_{Sh} \text{ Sin } \Theta \text{ d } \Theta}{\int_0^{\Theta_s} \text{ Sin } \Theta \text{ d } \Theta} \qquad \text{(T-8)}$$

$$\overline{N_{Nu}} = \int_0^{\Theta_s} \frac{N_{Nu}' \text{ Sin } \Theta \text{ d } \Theta}{\int_0^{\Theta_s} \text{ Sin } \Theta \text{ d } \Theta} \qquad \text{(T-9)}$$

where Θ_s is the flow separation angle.

It is required that the temperature field be established before the mass transfer rate is calculated to account for the effect of temperature on the physical properties. Equation (T-4) was thus solved first and the results so obtained were used to modify Pe_M in equation (T-3).

i) Numerical Solution

The complexity of the equations to be solved suggests that numerical, rather than analytical, techniques should be employed. The most straightforward of these numerical methods is that of finite differences, whereby derivatives are replaced by differences between adjacent point values (in a manner to be shown in the next section) to transform the partial differential equation into a set of linear algebraic equations. A method developed by Houghton (13) was used in this study with some modification.

To operate this method, space around the sphere under study must be divided and distinct point defined at which velocities and

system variables will be calculated. Figure (T-1) illustrates the manner in which the mesh was set up for this problem. The step size increases in the r-direction as r_i increases in the following way:

$$r_i = 1 + \frac{\Delta r_0 (h^{i-1} - 1)}{h - 1} \qquad \text{(T-4A)}$$

where h is a positive constant greater than 1

Δr_0 is the first radial increment (at the sphere surface)

The distance between adjacent points was controlled most directly by the choice of Δr_0 and the rate at which the distance between adjacent pairs of points increased was controlled by the size of h.

The reason for allowing the step size in the radial direction to vary within the mesh while the angular step size was fixed is connected with the gradients involved. Both the first and second derivatives with respect to radius of C and T changed very rapidly very close to the sphere surface and very slowly at large r. To use a very fine, constant step in the radial direction would adequately define the radial gradients, but prohibitive computation times would be involved unnecessarily at large r. The angular gradients change much more slowly with θ however and a constant step size was adequate.*

ii) Finite Difference Equations

As will be shown, a set of simultaneous linear agebraic equations is generated for both the heat transfer and the mass transfer problem at each value of the angle Θ. These equations form a

---

* It was found necessary to refine the angular step size at the frontal stagnation point to get the solution started with a minimum of oscillation.

tridiagonal banded matrix which can easily and rapidly be solved by Gaussian elimination. The values of concentration and temperature so calculated are used in the next step so that the solution "marches" through the profile from small to large values of the angle Θ.

a) Temperature profile:

In its dimensionless form the heat transfer equation (equation (T-4)) is:

$$V_r \frac{\partial T}{\partial r} + \frac{V_\Theta}{r} \frac{\partial T}{\partial \Theta} = \frac{2}{Pe_H} \left[\frac{\partial^2 T}{\partial r^2} + \frac{1}{r} \frac{\partial T}{\partial r} \right] \qquad (T\text{-}4)$$

In this equation the angular derivative was replaced by the forward difference approximation developed from the Taylor series expansion about T (i,j):

$$\left. \frac{\partial T}{\partial \Theta} \right|_{(i,j)} = \frac{T_{(i+1,j)} - T_{(i,j)}}{\Delta \Theta}$$

To aid in the stability of the solution, the radial derivatives were averaged between the i-th and the (i+1)th central difference steps:*

$$\left. \frac{\partial T}{\partial r} \right|_{(i,j)} = \frac{1}{2} \left[\left. \frac{\partial T}{\partial r} \right|_{(i,j)} + \left. \frac{\partial T}{\partial r} \right|_{(i+1,j)} \right]$$

$$= \frac{1}{2} \left[\frac{(T_{(i,j+1)} + T_{(i+1,j+1)}) - (T_{(i,j-1)} + T_{(i+1,j-1)})}{2 \Delta r_j} \right]$$

---

* The subscripts "i" increase with angle Θ and the subscripts "j" increase with radius.

$$\frac{\partial^2 T}{\partial r^2}\Big|_{(i,j)} = \frac{1}{2}\left[\frac{\partial^2 T}{\partial r^2}\Big|_{(i+1,j)} + \frac{\partial^2 T}{\partial r^2}\Big|_{(i,j)}\right]$$

$$= \frac{1}{2}\left[\frac{T_{(i+1,j+1)} + T_{(i,j+1)} - 2\,(T_{(i+1,j)} + T_{(i,j)}) + T_{(i+1,j-1)} + T_{(i,j-1)}}{\Delta r^2_j}\right]$$

Details of the above approximations are given in Appendix D. The above lead to the following finite difference equation when substituted into equation (T-4):

$$(a + b)\,(T(i+1,j+1) + T(i,j+1)) + (a - b)\,(T(i+1,j-1) + T(i,j-1)) - T(i,j) = (2a + 1)\,T(i+1,j) \qquad \text{(T-5)}$$

where $a = \dfrac{\Delta\Theta . r}{Pe_H (\Delta r)^2 . V_\Theta}$ $\qquad$ $b = \dfrac{\Delta\Theta}{Pe_H (\Delta r) . V_\Theta} - \dfrac{\Delta\Theta . r . V_r}{4(\Delta r) . V_\Theta}$

Development of (T-5) is left to Appendix E.

This is the point of departure from existing isothermal solutions of the transport process. In this study Pe_H was considered a variable of the system, depending on the temperature at that point. Its presence required the solution of equation (T-5) to be iterative.

The initial approximation to the temperature profile was conduction into a stagnant fluid, solving

$$\frac{\partial^2 T}{\partial r^2} = 0$$

with boundary conditions $\quad T = T_d$ at $r = 1$ $\quad$ and $\quad T = T_\infty$ at $r = \infty$

to give:

$$T_j = \frac{(T_d - T_\infty)(1 - r_j)}{r_j (1 - 1/R)} + T_d \qquad \text{(T-6)}$$

for all values of θ (i.e. all values of i)

At each mesh point Pe_H was calculated from the temperatures obtained in (T-6) and these used in (T-5) to solve for a new temperature profile. This process was repeated (calculation of local Pe_H from the temperature profile and re-substitution into (T-5) to improve the temperatures) until successive values of the temperature varies less than a specified amount.

Boundary Conditions

Because equation (T-4) is elliptic in r, two boundary conditions must be specified in the radial direction: the surface temperature was assumed to have a constant value T_d and the bulk fluid was assumed constant at T_∞.

In the θ-direction, the equation is parabolic requiring only one boundary condition, that at $\theta = 0$. The actual temperatures along the axis of symmetry ($\theta = 0$) need not be specified but it suffices to satisfy

$$\frac{\partial T}{\partial \theta} = 0$$

along $\theta = 0$. Finer divisions in the angular step size were chosen near $\theta = 0$ to aid in the satisfaction of this zero-slope condition.

Numerically, the condition was met by calculating values of C(2,j) and T(2,j) and comparing them to those of C(1,j) and T(1,j) respectively. If they differed more than a set amount (at the same

distance from the surface) the values for (2,j) were put into (1,j) and the process repeated until convergence occurred.*

b) Concentration Profile:

An entirely analagous finite difference equation was developed for the mass transfer problem and can be shown to be of the form:

$$(a + b)\,(C(i+1,j+1) + C(i,j+1)) + (a - b)\,(C(i+1,j-1) + C(i,j-1)) - C(i,j) = (2a + 1)\,C(i+1,j) \qquad \text{(T-7)}$$

with the initial approximation along $\Theta = 0$ derived from diffusion into a stagnant fluid. The boundary conditions are:

$$C_A = C_s \quad \text{at} \quad r = R$$

$$C_A = 1 \quad \text{at} \quad r = \infty$$

$$\frac{\partial C_A}{\partial \Theta} = 0 \quad \text{at} \quad \Theta = 0$$

The limitations of the ideal treatment generally must be mentioned. Thermal diffusion is neglected with respect to molecular diffusion. Isothermal fluid mechanics are applied to a highly non-isothermal system. In the short view these are not major shortcomings because the film temperature theories are no better in this respect. They are, however, problems which must be resolved if accurate fluxes are to be predicted.

---

* It was found that it was sufficient to only check the zero-slope criterion at the first five radial positions, creating a savings in computation time of roughly 30% where the resulting $\overline{N}_{Sh}$ changed by 10^{-3} in about 20.

The mass flux results apply only to spheres at a higher temperature than the bulk fluid, but this is a mechanical, rather than a fundamental limitation. The boundary conditions in the program could quite easily be changed to accommodate a cooler discontinuous phase.

It should be noted that although the finite difference calculations (equations (T-8) and T- 9)) involve angles only from the frontal stagnation point to the separation angle, ignoring the vortex region, Houghton (13) suggests that this is not a bad assumption, provided there is no vortex shedding. This is a result both of the small size of the vortex for the Reynolds numbers involved and the fact that the recirculating stream in the vortex region would tend to be depleted in the diffusing species. The effect of this assumption in this work was considered minimal because the highest Reynolds number used was 100, at which the separation angle was about 122^{o} from the frontal stagnation point. This might suggest that the predictions of flux (mass/unit time/unit surface) would be high by 180/122 but this is not likely the case. The low local Sherwood numbers in the vortex region would reduce the error considerably. It would be possible to remedy the situation, if it were felt necessary in other studies, by integrating from $\Theta = 0$ to $\Theta = \Theta_s$, and then calculating the velocities in the vortex region and integrating from $\Theta = \pi$ to $\Theta = \Theta_s$ to give an average Sherwood number in the vortex region.

Forced convection heat transfer data have been included in their raw form in Appendix J because they were needed to calculate the mass transfer results. They were not discussed at all because their importance changes with temperature relative to radiation and they cannot be

treated in a way analagous to that for mass transfer.

The finite difference calculations, and the empirical formula resulting from them represent a more realistic estimate of the mass flux than was previously available.

CHAPTER 3

RESULTS

This study concerned itself mainly with the mass transfer of an oxidizing gas from a low-temperature fluid steam to a high-temperature, reacting, spherical droplet. Convective heat transfer data was also obtained but will not be treated in any detail.

The parameters of interest in the study were bulk fluid flow rate (or, identically, velocity of the falling drop), temperature of the sphere under study (the temperature of the bulk fluid was usually held constant) and mole fraction of the oxidizing gas in the continuous phase. It is an attempt to check the validity of "film-temperature" approximations to this sort of flux calculation in the presence of large temperature gradients. The film temperature chosen as the basis for the isothermal approximations was the arithmetic mean film temperature:

$$T_f = \frac{T_d + T_\infty}{2}$$

The results of the finite difference calculations are given in Appendix J. The fluxes are calculated actually at the product of (flux) x (radius) because it is a slightly more general approach:

$$\text{flux} = - D_{AB} \cdot \frac{\partial C}{\partial r}$$

$$N_{Sh} = - 2 \frac{\partial C^*}{\partial r^*} \Bigg|_{r^* = 1}$$

$$\text{i.e.} \quad \text{flux} = \frac{1}{2} D_{AB} \cdot N_{Sh} \cdot \frac{[C(\text{bulk}) - C_s]}{R}$$

$$\text{or} \quad \text{flux} \cdot R = \frac{1}{2} D_{AB} \cdot N_{Sh} [C(\text{bulk}) - C_s] \qquad \text{(R-1)}$$

and this last form is independent of radius.

The mass transfer results for N_2 - O_2 mixtures are given in Table (R-1). The finite difference Sherwood numbers are quoted as $N_{Sh}(1)$ and the fluxes (for R = 0.1 cm.) are given by flux (1) of the Table. They are listed for the four different mole fractions in the gas mixture, the three Reynolds numbers, and all the drop temperatures used.

To examine the effect of the temperature gradients on the results, an "isothermal" calculation was carried out. Using the film temperature defined previously, the "isothermal" calculation assumes $T_d = T_\infty = T_f$ and calculates the flux again by the same finite difference formula. These Sherwood numbers and fluxes are $N_{Sh}(2)$ and flux (2) of Table (R-1).

Accepting for the moment that the calculation of fluxes using only T_f is a reasonable approximation (it will be dealt with in more detail later), the difference between fluxes (1) and (2) (see Figure (R-1) and (R-1A)) must be due to the effect of the temperature gradients, present in one and not the other. The temperature scales of Figures (R-1) and (R-1A) have been adjusted so that $(T_d - T_\infty)$ and the corresponding T_f occur above one another and when $(T_d - T_\infty) = 0$, $T_f = 350^oK.$, the bulk gas temperature.

It was hoped that the "isothermal" approach (giving flux (T_f)) would lead to greater simplification in the calculations than the "true"

TABLE R-1

D_p = 0.2 cm T_∞ = 350°K
N_2-O_2 mixture

X_{O_2}	Re	T_d	$T_d - T_\infty$	T_f	N_{Sh} (1)	N_{Sh} (2)	Flux(x10⁴ moles/cm²/sec) (1)	Flux(x10⁴ moles/cm²/sec) (2)	Flux(x10⁴ moles/cm²/sec) (3)
0.2	10	2000	1650	1175	8.07	7.85	18.58	2.04	2.01
		1800	1450	1075	8.09	7.87	15.37	1.90	1.88
		1600	1250	975	8.11	7.89	12.43	1.76	1.74
		1400	1050	875	8.13	7.93	9.77	1.62	1.60
		1200	850	775	8.16	7.97	7.41	1.48	1.45
		1000	650	675	8.20	8.03	5.33	1.33	1.31
		800	450	575	8.25	8.11	3.57	1.17	1.16
		600	250	475	8.30	8.21	2.13	1.02	1.00
	50	2000	1650	1175	14.53	14.11	33.44	3.68	3.62
		1800	1450	1075	14.56	14.15	27.67	3.42	3.38
		1600	1250	975	14.60	14.20	22.38	3.17	3.13
		1400	1050	875	14.65	14.26	17.61	2.91	2.87
		1200	850	775	14.71	14.35	13.35	2.66	2.61
		1000	650	675	14.78	14.47	9.62	2.39	2.35
		800	450	575	14.82	14.62	6.44	2.12	2.08
		600	250	475	14.98	14.81	3.84	1.84	1.80
	100	2000	1650	1175	22.28	21.63	51.30	5.64	5.55
		1800	1450	1075	22.34	21.69	42.44	5.24	5.17
		1600	1250	975	22.41	21.76	34.34	4.86	4.79
		1400	1050	875	22.49	21.87	27.02	4.47	4.60
		1200	850	775	22.49	22.01	20.49	4.08	4.01
		1000	650	675	22.70	22.20	14.77	3.67	3.61
		800	450	575	22.85	22.44	9.90	3.25	3.20
		600	250	475	23.03	22.17	5.91	2.82	2.77

(1) using $T_d > T_\infty > T_f$ (2) using $T_d = T_\infty = T_f$ (3) using T_f and film temperature approximation (11)

TABLE R-1 (continued)

X_{O_2}	Re	T_d	T_d-T_∞	T_f	N_{Sh} (1)	N_{Sh} (2)	Flux($\times 10^4$ moles/cm^2/sec) (1)	Flux($\times 10^4$ moles/cm^2/sec) (2)	Flux($\times 10^4$ moles/cm^2/sec) (3)
0.4	10	2000	1650	1175	8.16	7.92	37.55	4.14	4.07
		1800	1450	1075	8.17	7.94	31.06	3.85	3.78
		1600	1250	975	8.20	7.97	25.12	3.56	3.51
		1400	1050	875	8.22	8.01	19.76	3.27	3.23
		1200	850	775	8.25	8.06	14.98	2.98	2.94
		1000	650	675	8.29	8.12	10.79	2.69	2.64
		800	450	575	8.34	8.20	7.22	2.38	2.34
		600	250	475	8.40	8.31	4.31	2.06	2.02
	50	2000	1650	1175	14.69	14.23	67.64	7.45	7.31
		1800	1450	1075	14.73	14.30	55.96	6.92	6.82
		1600	1250	975	14.77	14.35	45.28	6.41	6.32
		1400	1050	875	14.82	14.42	35.62	5.90	5.81
		1200	850	775	14.89	14.51	27.01	5.38	5.29
		1000	650	675	14.96	14.63	19.47	4.84	4.76
		800	450	575	15.05	14.79	13.04	4.29	4.22
		600	250	475	15.17	14.99	7.78	3.72	3.65
	100	2000	1650	1175	22.55	21.86	103.82	11.38	11.22
		1800			22.61	21.92	85.91	10.60	10.46
		1600			22.68	22.01	69.53	9.84	9.69
		1400			22.77	22.13	54.71	9.05	8.91
		1200			22.87	22.28	41.49	8.25	8.12
		1000			22.99	22.47	29.92	7.43	7.31
		800			23.14	22.73	20.05	6.59	6.48
		600			23.33	23.06	11.96	5.71	5.62

TABLE R-1 (continued)

X_{O_2}	Re	T_d	T_d-T_∞	T_f	N_{Sh} (1)	N_{Sh} (2)	Flux($\times 10^4$ moles/cm^2/sec) (1)	Flux($\times 10^4$ moles/cm^2/sec) (2)	Flux($\times 10^4$ moles/cm^2/sec) (3)
0.6	10	2000	1650	1175	8.24	8.00	56.90	6.25	6.16
		1800			8.26	8.02	47.07	5.82	5.74
		1600			8.28	8.05	38.08	5.40	5.32
		1400			8.31	8.09	29.96	4.96	4.89
		1200			8.34	8.14	22.70	4.55	4.45
		1000			8.38	8.20	16.36	4.07	4.00
		800			8.43	8.29	10.96	3.60	3.54
		600			8.49	8.40	6.53	3.12	3.07
	50	2000			14.85	14.40	102.57	11.20	11.09
		1800			14.89	14.44	84.87	10.50	10.33
		1600			14.94	14.50	68.68	9.72	9.57
		1400			14.99	14.58	54.04	8.94	8.81
		1200			15.06	14.67	40.98	8.15	8.02
		1000			15.14	14.80	29.54	7.34	7.22
		800			15.23	14.96	19.79	6.51	6.40
		600			15.35	15.17	11.80	5.64	5.54
	100	2000			22.81	22.09	157.54	17.25	17.01
		1800			22.88	22.16	136.37	16.1	15.86
		1600			22.96	22.26	105.53	14.9	14.70
		1400			23.04	22.38	83.05	13.7	13.52
		1200			23.15	22.54	62.99	12.5	12.32
		1000			23.27	22.74	45.43	11.3	11.10
		800			23.43	23.01	30.45	10.0	9.84
		600			23.63	23.35	18.17	8.68	8.53

TABLE R-1 (continued)

X_{O_2}	Re	T_d	T_d-T_∞	T_f	N_{Sh} (1)	N_{Sh} (2)	Flux($\times 10^4$ moles/cm^2/sec) (1)	Flux($\times 10^4$ moles/cm^2/sec) (2)	Flux($\times 10^4$ moles/cm^2/sec) (3)
0.8	10	2000	1650	1175	8.32	8.07	76.62	8.40	8.28
		1800	1450	1075	8.34	8.09	63.40	7.84	7.72
		1600	1250	975	8.37	8.13	51.30	7.26	7.16
		1400	1050	875	8.40	8.17	40.35	6.68	6.58
		1200	850	775	8.43	8.22	30.59	6.09	5.99
		1000	650	675	8.47	8.29	22.05	5.48	5.39
		800	450	575	8.52	8.38	14.76	4.86	4.78
		600	250	475	8.58	8.49	8.80	4.21	4.13
	50	2000			15.01	14.53	138.22	15.1	14.92
		1800			15.05	14.58	114.38	14.1	13.91
		1600			15.10	14.65	92.58	13.1	12.90
		1400			15.16	14.73	72.85	12.0	11.86
		1200			15.23	14.83	55.25	11.0	10.81
		1000			15.31	14.96	39.84	9.90	9.73
		800			15.40	15.13	26.69	8.77	8.63
		600			15.53	15.35	15.92	7.61	7.48
	100	2000			23.07	22.31	212.42	23.2	22.90
		1800			23.14	22.39	175.82	21.7	21.36
		1600			23.22	22.50	142.33	20.1	19.81
		1400			23.31	22.63	112.03	18.5	18.23
		1200			23.42	22.80	84.99	16.9	16.62
		1000			23.55	23.01	61.30	15.2	14.97
		800			23.72	23.28	41.09	13.5	13.27
		600			23.92	23.64	24.53	11.7	11.51

calculations (giving flux (T_d)) so an attempt was made to correlate the two. After some trial and error, the relationship chosen was:

$$\text{Flux } (T_d) = \text{Flux } (T_f) \cdot A \cdot \frac{T_f}{T_\infty} \cdot \left(\frac{T_d}{T_\infty}\right)^B \qquad \text{(R-3)}$$

which can be shown* to be equivalent to:

$$\text{Flux } (T_d) = \text{Flux } (T_f) \cdot A \cdot \left(\frac{x+1}{2}\right) \left(\frac{2x}{x+1}\right)^B \qquad \text{(R-4)}$$

$$\text{if } x = T_d/T_\infty$$

To evaluate constants A and B, the fluxes (1) and (2) from Table (R-1) (for N_2-O_2) mixtures only) were compared. Taking logs in equation (R-4) gives:

$$\log \left[\frac{\text{Flux } (T_d)}{\text{Flux } (T_f)} \times \frac{2}{x+1} \right] = \log A + B \log \left(\frac{2x}{x+1}\right) \qquad \text{(R-5)}$$

When the ordinary least-squares line (assuming normal error distribution) is calculated from the data of Table (R-1) and equation (R-5), A and B can be evaluated.

The result of this calculation is shown in Table (R-2). In each prediction of A and B the correlation coefficient was better than 0.999 for six degrees of freedom (calculations were done for 8 temperatures for each value of A and B). Using the average values of A and B from Table (R-2) the prediction becomes:

$$\text{Flux } (T_d) = 0.988 \text{ Flux } (T_f) \times \frac{(T_d/T_\infty + 1)}{2} \times \left(\frac{2\, T_d/T_\infty}{T_d/T_\infty + 1}\right)^{1.902} \qquad \text{(R-6)}$$

---

* See Appendix H

Because of the size of σ_A and σ_B, prediction of A and B to 95% confidence ($\pm 3\sigma$) is just as justified using B = 2; A = 1 (and, indeed, by setting $T_d = T_\infty$ in equation (R-6), flux (T_d) becomes equal to flux (T_f) and A = 1 is shown to be an identity) giving the following:

$$\text{Flux } (T_d) = \frac{2x^2}{(x+1)} \cdot \text{Flux } (T_f) \qquad \text{(R-7)}$$

but better agreement was found using:

$$\text{Flux } (T_d) = \text{Flux } (T_f) \cdot \frac{1.87x^2}{(x+1)} \qquad \text{(R-8)}$$

Because of the complex calculations involved in both flux (T_d) and flux (T_f) there would be little purpose in establishing the correlation if there were not a simpler way of calculating one of the fluxes. Hamielec, Lu and McLean* (11) have suggested, for the same definition of T_f that the mass flux might be approximated by:

$$\text{Flux (FTA**)} = \frac{N_{Sh_f} \cdot D_{AB_f} \cdot P}{D_p . R . T_f} \cdot Y \text{ (oxidizing gas)} \qquad \text{(R-9)}$$

where, in the presence of large thermal gradients, physical properties are evaluated at the arbitrary film temperature T_f.

Table (R-3) shows the comparison between the fluxes (T_f) by finite differences and those by the film temperature approximation for the same T_f. The agreement is better than 2%, considered to be within

---

* See Appendix F

** "Film Temperature Approximation"

TABLE R-2

N_2 - O_2 mixture
D_p = 0.2 cm.

X_{O_2}	Re	B	A
0.2	10	1.899	0.988
	50	1.904	0.986
	100	1.897	0.990
0.4	10	1.899	0.988
	50	1.896	0.989
	100	1.901	0.989
0.6	10	1.894	0.990
	50	1.908	0.986
	100	1.907	0.988
0.8	10	1.905	0.987
	50	1.913	0.985
	100	1.905	0.989

$\overline{B}$ = 1.902 $\quad\quad$ σ_B = 0.048

$\overline{A}$ = 0.988 $\quad\quad$ σ_A = 0.029

the total accuracy of the calculations. The Sherwood number used by Hamielec et al. is that of the Ranz-Marshall correlation, but here, that predicted by finite differences was used in equation (R-9) for better self-consistency in the calculations (to ensure that no differences in flux would arise through different ways of choosing the Sherwood numbers.).

The close agreement between the two methods means that the flux (FTA), which is very easy to calculate, can be used in place of the finite difference flux (T_f) of equation (R-8):

$$\text{Flux } (T_d) = \frac{1.87\ x^2}{(x + 1)} \cdot \text{Flux (FTA)} \qquad \text{(R-10)}$$

To check to predictability of equation (R-10), Table (R-4) was assembled. Flux (1) represents flux (FTA) and flux (2) the result of applying equation (R-10) to flux (1). Flux (3) is the finite difference solution, representing the "true" flux.

For the N_2 - O_2 mixtures, agreement is better than 5% in all but one case, and for the greatest differences between T_d and T_∞ it is better than 3%. The agreement could be improved to between 1% and 2% by using B = 1.902 as originally calculated, but at the expense of slightly more calculation effort.

Although the values of B in equations (R-6) and (R-7) were determined only for N_2 - O_2 mixtures, the same values worked quite well for both N_2 - CO_2 and He - O_2 mixtures, as the rest of Table (R-4) illustrates.

When flux (FTA) was plotted against temperature as in Figures (R-2A) through (R-2D), values could be interpolated for temperatures other than those calculated, and from these, "true" fluxes could be calculated. These

TABLE R-3

D_p = 0.2 cm.

N_2 - O_2 mixture

Re	X_{O_2}	$T_d(^oK)$	$T_f(^oK)$	Flux ($\times 10^4$) moles/cm^2/sec (A)	(B)
10	0.2	2000	1175	2.04	2.01
		1800	1075	1.90	1.88
		1600	975	1.76	1.74
		1400	875	1.62	1.60
		1200	775	1.48	1.45
		1000	675	1.33	1.31
		800	575	1.17	1.16
		600	475	1.02	1.00
100	0.8	2000	1175	23.2	22.9
		1800	1075	21.7	21.4
		1600	975	20.1	19.8
		1400	875	18.5	18.2
		1200	775	16.9	16.6
		1000	675	15.2	15.0
		800	575	13.5	13.3
		600	475	11.7	11.5

(A) T_f finite difference calculations

(B) Film Temperature Approximation (11)

TABLE R-4

N_2 - O_2

D_p = 0.2 cm

Oxidizing Mole fr'n.	Re	T_d	Flux ($\times 10^4$ moles/cm^2/sec) (1)	(2)	(3)	Ratio (2)/(3)
0.2	10	2000	2.01	18.23	18.58	0.981
		1800	1.88	15.15	15.37	0.986
		1600	1.74	12.20	12.43	0.981
		1400	1.60	9.57	9.77	0.980
		1200	1.45	7.19	7.41	0.970
		1000	1.31	5.19	5.33	0.973
		800	1.16	3.42	3.57	0.958
		600	1.00	2.02	2.13	0.948
0.8	100	2000	22.90	207.7	212.4	0.978
		1800	21.36	172.2	175.8	0.980
		1600	19.81	138.9	142.3	0.976
		1400	18.23	109.0	112.0	0.973
		1200	16.62	82.44	84.99	0.970
		1000	14.97	59.28	61.30	0.967
		800	13.27	39.15	41.09	0.953
		600	11.51	23.25	24.53	0.948
N_2 - CO_2						
0.2	10	2000	1.66	15.06	15.07	0.999
		1800	(1.55)	(14.06)		
		1600	1.43	10.02	10.09	0.993
		1400	(1.32)	(9.25)		
		1200	1.20	5.95	6.02	0.988
		1000	(1.07)	(4.24)		
		800	(0.95)	(2.80)		
		600	0.825	1.67	1.73	0.965
0.8	100	2000	18.21	165.16	168.74	0.979
		1800	(17.15)	(138.23)		
		1600	15.82	110.90	113.20	0.978
		1400	(14.60)	(87.31)		
		1200	13.33	66.12	67.65	0.977
		1000	(12.00)	(47.52)		
		800	(10.70)	(31.57)		
		600	9.31	18.81	19.54	0.963

(1) By equation (R-2)
(2) By equation (R-8)
(3) "True" flux from finite difference solution

TABLE R-4 (continued)

Oxidizing Mole fr'n.	Re	T_d	Flux ($\times 10^4$ moles/cm^2/sec) (1)	(2)	(3)	Ratio (2)/(3)
O_2 - He						
0.2	10	2000	5.96	54.06	54.33	0.995
		1800	(5.5)	(44.33)		
		1600	5.17	36.24	36.48	0.993
		1400	(4.65)	(27.81)		
		1200	4.35	21.59	21.83	0.989
		1000	(3.8)	(15.05)		
		800	(3.4)	(10.03)		
		600	3.02	6.10	6.32	0.965
0.8	10	2000	23.21	210.5	215.09	0.979
		1800	(21.7)	(174.90)		
		1600	20.07	140.7	143.74	0.979
		1400	(18.5)	(110.6)		
		1200	(16.9)	(83.8)		
		1000	(16.3)	(60.6)		
		800	(13.65)	(40.27)		
		600	(12.05)	(24.34)	24.42	0.997

are the values in parentheses in Table (R-4). Only extremes in mole fraction and Reynolds number are given in Table (R-4) but there were no anomalies detected in any other cases examined.

It is therefore possible to accurately predict mass flux in the presence of large temperature gradients by use of the simple formula:

$$\text{Flux} = \frac{1.87\ x^2}{(x + 1)} \cdot \frac{N_{Sh_f} \cdot D_{AB_f} \cdot P}{D_p \cdot RT_f} Y \text{ (oxidizer)} \qquad \text{(R-11)}$$

$$\text{where } x = T_d/T_\infty$$

That the finite difference mesh size had no effect on the calculations is shown in Table (R-5). Varying h* to move the outer boundary, and $\Delta\Theta$* to change the number of angular steps shown that the combination

$$h = 1.3 \qquad \Delta r_o = 5 \times 10^{-5} \qquad \Delta\Theta = 3.6^o$$

includes no detectable boundary effects.

The finite difference solutions were solved in terms of Reynolds numbers so as to be independent of drop diameter**. Radius was introduced later for comparison with the film-temperature approximations.

Figures (R-3) and (R-4) show typical concentration and temperature profiles. Because the Sherwood and Nusselt numbers vary so little with temperature (Figure (R-5)) it is possible to use the values for the bulk gas temperature (T_∞) (at which Re is usually given).

---

* In equation (T-4A)

** See Appendix G

TABLE R-5

h	Δr_o	R_{max}	$\Delta\Theta$	$\overline{N}_{Nu}$	Heat Flux * radius	$\overline{N}_{Sh}$	Mass Flux * radius
1.10	5×10^{-5}		3.6^o	No convergence on $\frac{\partial c}{\partial \Theta}$ *			
1.15	5×10^{-5}	1.089	3.6^o	24.4827	4.9650	23.7979	4.1572×10^{-4}
1.20	5×10^{-5}	1.37	3.6^o	8.9319	1.8113	8.8047	1.5381
1.25	5×10^{-5}	2.50	3.6^o	8.7741	1.7794	8.6164	1.5052
1.30	5×10^{-5}	7.02	3.6^o	8.7775	1.7800	8.6277	1.5072
1.30	5×10^{-5}	7.02	6^o	8.7831	1.7812	8.6138	1.5047

CO_2 - N_2

$X_{CO_2} = 0.2$

$Re = 10$

$T_d = 2000^oK$

$T_\infty = 350^oK$

* 50 iterations to 0.005 tolerance

CHAPTER 4

DISCUSSION

This work represents an attempt to more accurately estimate the mass flux to or from the surface of a hot sphere from or to a bulk fluid phase at a lower temperature. Most of the discussion so far has centered around flux to the surface of the drop but with the dimensionless concentration defined as:

$$C^* = \frac{C - C_s}{C_\infty - C_s}$$

It can be seen that the values of C^* are the same whether C_s is larger than C_∞ or vice versa (that is, whether diffusion is to the sphere or away from it). This means that the dimensionless profile is unchanged, as are the dimensionless gradients $\frac{\partial C^*}{\partial r^*}$. The only thing that changes is that in Equation (R-1) the difference (C(bulk) - C_s) changes sign, changing the sign of the flux, indicating that the material flow is in the opposite direction. The solution as developed, however, holds only for systems in which the continuous phase is at a lower temperature than the discontinuous phase. To reverse the situation and make the drops cooler than the bulk fluid is straightforward; simply being a matter of resolving the energy equation with the boundary conditions of temperature reversed. This will affect the transport properties and so the mass fluxes will be different under identical flow conditions to the first case mentioned ($T_d > T_\infty$).

The discrepancy between these results and those using the film-temperature approximations, even at fairly small temperature differences requires that a re-evaluation of the film-temperature approach be made.

Looking at Figures (R-1) and (R-1A) (the latter being merely an amplification of (R-1) for small values of the temperature difference) one can see that the error made by the film-temperature approximation (when compared to the results of Equation (R-11)) has reached nearly 50% by the time the temperature difference is 200°K. The error is nearly 15% even at temperature differences as small as 50°K. This information, and that in Figure (R-1A) might provide some guide to the accuracy one might expect if it were found desirable to continue using the simple film-temperature approximation. Since the correction involved in the use of Equation (R-11) is significant and involves very little additional work, it is recommended that it be used in all cases where the film-temperature approximation might have been used formerly.

The model has been tested with drop temperatures from 351°K to 2000°K over a wide range of concentrations and for Reynolds numbers ranging from 10 to 100. The binary gas mixtures used were: N_2 - O_2, N_2 - CO_2, and He - O_2; all calculations being carried out assuming a bulk gas temperature of 350°K and 1 atmosphere pressure. The inclusion of helium - oxygen mixtures was mainly for the purpose of testing the model under what were considered extreme conditions - helium having such grossly different properties than any of the other gases.

Extrapolation of the model to very high or very low pressures was not attempted because the form used for the molecular diffusivity in the

finite difference equations is valid only at atmospheric pressure. The extension of these calculations into ternary mixtures and higher should be possible provided the diffusivity can be evaluated.

In a theoretical treatment such as this it is usually most advisable to have experimental corroboration for the results presented. This was not done in this work because of the difficulty in interpreting data in the literature (4) in terms of the parameters needed in this study. Because of the direct relationship between temperature and flux in the model (D_{AB} varies as the 1.8 power of T and the flux varies directly with D_{AB}) a very good estimate of the temperature of the drop must be obtained. The highly exothermic reactions associated with impurity oxidation in iron refining cause the drop to heat up a great deal during the first portion of free fall. This makes any measurement of the temperature in the melting zone a very crude estimate of the actual temperature during the fall. A good estimate of the flux also requires accurate knowledge of the temperature gradient around the drop because of the temperature dependence of the transport parameters. Figure (R-3) shows how steep the temperature gradient is in the model (which assumes that there is no secondary reaction such as the burning of CO to CO_2 in the continuous phase). The existence of a large flame envelope around the drop in experimental studies makes it extremely difficult to estimate the bulk temperature that should be used in the calculations. It is certainly no longer the temperature of the input gas stream. Until experiments can be specifically designed to adequately measure these parameters, correlation with experiment is of little value. Hamielec et a. (11) have reported quite good

agreement with experimental work with a film-temperature calculation and their results are in poor agreement with the results of this study. It should be pointed out that Hamielec et al. (11) interpreted the data in the literature based on the same assumption used by previous workers in this field that the rate of reaction is solely controlled by mass transfer in gas phase. The present study predicts a significantly higher mass transfer rate than that obtained by using film-temperature approximation and the experimental data. Besides the uncertainty in the estimation of bulk gas temperature, it would be reasonable to question the validity of the generally accepted assumption that the overall rate is controlled solely by mass transfer in the gas phase. Further discussion on this matter is beyond the scope of the present study.

The large difference which exists between the film-temperature results and the more accurate ones calculated here seems to come from the differing evaluation of two terms. While both methods, for the same values of the Sherwood number ($-\frac{2\partial C^*}{\partial r^*}$) define the flux by:

$$\text{Flux} = -D_{AB}\frac{C}{r}$$

$$= -2\frac{D_{AB}.C}{D_p}\cdot\frac{\partial C^*}{\partial r^*}$$

$$= \frac{N_{Sh}.D_{AB}.C}{D_p} \qquad \text{(D-1)}$$

(assuming the concentration of diffusing species on the sphere surface to be zero), the film-temperature calculation evaluates both D_{AB} and C at T_f. The finite difference approximation calculates the diffusivity at the drop

temperature (T_d) and the concentration at the bulk temperature (T_∞). For $T_d = 2000^oK$, $T_f = 1175^oK$, $T_\infty = 350^oK$ this means that D_{AB} evaluated at T_d is about three times that at T_f and the concentration of diffusing species at T_∞ is about three times that at T_f. This leads to a discrepancy in the flux calculations that is worst when T_d is much higher than T_∞.

This difference in formulation and that Sherwood number is insensitive to temperature (Fig. (R-5)) led to the suggestion, very late in the analysis, that a possible equation for the flux calculation might be:

$$\text{Flux} = \frac{N_{Sh} \cdot D_{AB_{Td}} \cdot C_{\infty_{T\infty}}}{D_p} \qquad \text{(D-2)}$$

Results using this equation are as follows:

$D_p = 0.2$ cm. Re = 10

$T_d = 2000^oK$ N_2 - 20% O_2

Flux (D-2) = 18.1×10^{-4} moles/cm^2/sec

Flux (R-8) = 18.23×10^{-4} moles/cm^2/sec

$T_d = 600^oK$

Flux (D-2) = 2.38×10^{-4} moles/cm^2/sec

Flux (R-8) = 2.02×10^{-4} moles/cm^2/sec

No recommendation will be made about the range of usefulness of equation (D-2) because it has had very little testing but does seem in some cases to be a viable alternative to Equation (R-11).

Because, as Figure (R-5) indicates, the Sherwood number is fairly insensitive to changes in temperature, the evaluation of it can be any temperature at which it is convenient to evaluate the relevant parameters.

It should be noted that the Sherwood numbers used in the approximate calculations in this study were actually those calculated by the finite difference programs. This was done to ensure that the results would differ only because of the different assumptions they made about the way in which the temperature affected the transport process. It must be realized that if correlations such as that of Ranz-Marshall are used to predict the Sherwood numbers for use in the flux calculations that they can independently introduce inaccuracies.

Overall, the results of this study indicate that the method of calculating flux in the presence of large temperature gradients has, up to the present, been inadequate; especially as the difference between temperatures of the bulk fluid and discontinuous phase increases. Although this effort has been largely interested in the resolution of problems associated with the oxidation of impurities from liquid iron, the results have been presented in such a way, and over such a range of temperatures, that it is hoped that they might find use in many other areas.

Some of the uses to which a study such as that undertaken here might be put include the following. Because of the heating of the gas around the flowing stream in spray refining, the temperature gradients between the gas and the drop which exist in the spray tower are probably considerably reduced. This, as shown above, would reduce the flux of oxygen to the surface of the drops, cutting down the refining rate. By estimating the Sherwood number by the Ranz-Marshall correlation (bearing in mind the possible inaccuracies mentioned earlier) it is possible to calculate N_{Sh} and so the flux as a function of time for a free-falling

drop. This is because the evaluation of the Reynolds number for the correlation can, through the drag coefficient, be done as either a function of time or fall height. This would make it possible to estimate the optimum height of the tower for a given amount of refining.

The concepts, and indeed the calculations, with minor modifications might be used to estimate the rate of reoxidation during pouring, teeming and stream de-gassing. The dimensionless nature of the basic calculations means that they are not restricted to gas-liquid systems but might be applied to slag-metal reactions or the growth of spherical inclusions in a melt. These mention only a few areas of interest to metallurgists to which this type of calculation can be applied.

Thus a better understanding of some metallurgical problems can be gained by using concepts familiar to chemical engineers and the tools of the applied mathematician.

BIBLIOGRAPHY

1. Anon. Metallurgia 74, 197 (1966).
2. Anon. Iron and Steel 507-510 (1966).
3. Aziz, K., Hellums, J. D., Physics of Fluids, No. 2, 10, 314-324 (1967).
4. Baker, R., JISI, 205, 637-641 (1967); ibid. 239, 857-864 (1967); Baker, L. A., Warner, N. A., Jenkins, A. E. Trans. AIME 230, 1228-1235 (1964).
5. Bird, R. B., Stewart, W. E., Lightfoot, E. N., "Transport Phenomena" John Wiley and Sons, New York (1960).
6. Chucher, T. C., JISI, 200, 891 (1962).
7. Churchill, S. W., Brier, J. C., Chem. Eng. Prog. Symposium Series No. 17, 51 (1955).
8. Davies, D. R. G., Rhydderch, M. J., Shaw, L. J., JISI 205, 810-813 (1967).
9. Douglas, W. J. M., Churchill, S. W., Chem. Eng. Prog. Symposium Series No. 18, 52, 23 (1956).
10. Hamielec, A. E., Johnson, A. I., Can. J. Chem. Eng. 40, 41 (1962).
11. Hamielec, A. E., Lu, W.-K., McLean, A., Can. Met. Quarterly, No. 1, 7, 27-33 (1968).
12. Hamielec, A. E., Storey, S. H., Whitehead, J. M., Can. J. Chem. Eng. 41, 246 (1963).
13. Houghton, W. T., Ph.D. Thesis, McMaster University (1966).
14. McAdams, W. H., "Heat Transmission", p. 224, McGraw-Hill Book Company, New York (1933).
15. Johnson, A. I. Akehata, T., Can. J. Chem. Eng., 43, 10 (1965).

Bibliography (continued)

16. Rhydderch, M. J., JISI 205, 814-818 (1967).

17. Sheehan, W. F., "Physical Chemistry", p. 137, Allyn and Bacon, Boston (1961).

APPENDIX A

DERIVATION OF THE CONVECTION EQUATION FOR INCOMPRESSIBLE, AXISYMMETRIC FLOW (CONSTANT D_{AB})

Making a mass balance on Figure (A-1):

a) Transfer in the angular direction

Face 1-2: Area = $2\pi r \sin\Theta\, dr$

$$2\pi r \sin\Theta\, dr \cdot C_A \cdot V_\Theta - 2\pi r \sin\Theta\, dr \cdot \frac{D_{AB}}{r} \frac{\partial C_A}{\partial \Theta} \qquad \text{(A-1)}$$

where the first term represents convection at a volumetric flow rate V_Θ and the second term represents molecular diffusion from Fick's first law, the gradient in arc length $\frac{\partial C_A}{\partial s}$ having been replaced by $\frac{1}{r} \cdot \frac{\partial C_A}{\partial \Theta}$ by the identity $ds = r.d\Theta$

Face 3-4: Area = $2\pi r. \sin(\Theta + d\Theta) . dr$

$$2\pi r. \sin(\Theta + d\Theta) . dr. \left(C_A + \frac{\partial C_A}{\partial \Theta} \cdot d\Theta\right)\left(V_\Theta + \frac{\partial V_\Theta}{\partial \Theta}\, d\Theta\right)$$

$$- 2\pi r. \sin(\Theta + d\Theta) . dr. \frac{D_{AB}}{r} \cdot \left(\frac{\partial C_A}{\partial \Theta} + \frac{\partial^2 C_A}{\partial \Theta^2} \cdot d\Theta\right) \qquad \text{(A-2)}$$

and if $\sin(\Theta + d\Theta) = \sin\Theta + \frac{\partial(\sin\Theta)\, d\Theta}{\partial\Theta}$ (to first order)

$$= \sin\Theta + \cos\Theta . d\Theta$$

(A-2) can be written as

$$(\text{Sin}\theta + \text{Cos}\theta\, d\theta)\ (2\pi r.dr.\ (C_A + \frac{\partial C_A}{\partial \theta}\, d\theta)\ (V_\theta + \frac{\partial V_\theta}{\partial \theta}\, d\theta)\ )$$

$$- (\text{Sin}\theta + \text{Cos}\theta\, d\theta)\ (2\pi r.dr.\ \frac{D_{AB}}{r} \cdot (\frac{\partial C_A}{\partial \theta} + \frac{\partial^2 C_A}{\partial \theta^2} \cdot d\theta\ )\ ) \qquad \text{(A-3)}$$

The net angular flow, equal to the difference between (A-3) and (A-1) can be shown to be:

$$C_A\ (\frac{1}{r} \cdot \frac{\partial V_\theta}{\partial \theta} + \frac{\text{Cot}\theta}{r} \cdot V_\theta) + \frac{V_\theta}{r}\frac{\partial C_A}{\partial \theta} - D_{AB}\ (\frac{1}{r^2} \cdot \frac{\partial^2 C_A}{\partial \theta^2} + \frac{\text{Cot}\theta}{r^2}\frac{\partial C_A}{\partial \theta}) \qquad \text{(A-4)}$$

b) Transfer in the radial direction

<u>Face 2-3:</u> Area = $2\pi(r^2).\text{Sin}\theta\, d\theta$

$$2\pi r^2\ \text{Sin}\theta\, d\theta.\ C_A.V_r - 2\pi r^2\ \text{Sin}\theta\, d\theta.\ D_{AB} \cdot \frac{\partial C_A}{\partial r} \qquad \text{(A-5)}$$

<u>Face 1-4:</u> Area = $2\pi(r^2 + 2r.dr)\ \text{Sin}\theta\, d\theta$

$$2\pi(r^2 + 2r.dr)\ \text{Sin}\theta\, d\theta.\ (V_r + \frac{\partial V_r}{\partial r} \cdot dr)\ (C_A + \frac{\partial C_A}{\partial r} \cdot dr)$$

$$- 2\ (r^2 + 24.dr)\ \text{Sin}\theta\, d\theta.\ D_{AB} \cdot (\frac{\partial C_A}{\partial r} + \frac{\partial^2 C_A}{\partial r^2} \cdot dr) \qquad \text{(A-6)}$$

From the difference between (A-5) and (A-6) the net flow in the radial direction can be shown to be:

$$C_A\ (\frac{\partial V_r}{\partial r} + \frac{2V_r}{r}) \cdot + V_r \cdot \frac{\partial C_A}{\partial r} - D_{AB}\ (\frac{\partial^2 C_A}{\partial r^2} + \frac{2}{r} \cdot \frac{\partial C_A}{\partial r}\ ) \qquad \text{(A-7)}$$

Under steady state, net flow = 0*

$$\text{i.e. } V_r \frac{\partial C_A}{\partial r} + \frac{V}{r} \cdot \frac{\partial C_A}{\partial \Theta} = D_{AB} \left(\frac{\partial^2 C_A}{\partial r^2} + \frac{2}{r} \cdot \frac{\partial C_A}{\partial r} + \frac{\cot}{r^2} \cdot \frac{\partial C_A}{\partial \Theta} \cdot + \frac{1}{r^2} \cdot \frac{\partial^2 C_A}{\partial \Theta^2} \right) \tag{A-8}$$

which is the required convection equation.

---

* The continuity equation for these conditions is:

$$\frac{\partial V_r}{\partial r} + \frac{2V_r}{r} + \frac{2}{r} \frac{\partial V\Theta}{\partial \Theta} + \frac{\cot\Theta}{r} V_\Theta = 0$$

assuming steady-state ($\frac{\partial}{\partial t} = 0$), axisymmetric ($\frac{\partial}{\partial \Phi} = 0$), incompressible ($\frac{\partial \rho}{\partial r}, \frac{\partial \rho}{\partial \Theta} = 0$) flow. This equation leads to simplification in the (net flow = 0) leading to (A-8).

APPENIX B

EFFECT OF VARIATION OF D_{AB}, α WITH POSITION

The continuity equation (T-2) is strictly correct only if D_{AB} is not a function of (r,Θ). The portion of the equation written as

$$D_{AB}\left(\frac{\partial^2 c}{\partial r^2}+\frac{2}{r}\frac{\partial c}{\partial r}\right) \qquad \text{(B-1)}$$

is actually

$$D_{AB}\left(\frac{\partial^2 c}{\partial r^2}+\frac{2}{r}\frac{\partial c}{\partial r}\right)+\frac{\partial c}{\partial r}\cdot\frac{\partial D_{AB}}{\partial r} \qquad \text{(B-2)}$$

which comes from

$$\frac{1}{r^2}\frac{\partial}{\partial r}\left(r^2 D_{AB}\frac{\partial c}{\partial r}\right) \qquad \text{(B-3)}$$

for $D_{AB} = D_{AB}(r,\Theta)$, as (B-1) is developed for D_{AB} constant. Putting numbers from a typical solution of (T-2) into (B-2) shows for

$\Theta = 40^{o}$ $\qquad$ $r = 1$

$Re = 100$ $\qquad$ $T_s = 1800^{o}K$

$T_\infty = 350^{o}K$

$$D_{AB}\left(\frac{\partial^2 c}{\partial r^2}+\frac{1}{r}\frac{\partial c}{\partial r}\right) \approx 8 \times 10^{5}$$

and

$$\frac{\partial c}{\partial r}\cdot\frac{\partial D_{AB}}{\partial r} \approx 2.4 \times 10^{2}$$

This justifies dropping the terms in $\frac{\partial c}{\partial r} \cdot \frac{\partial D_{AB}}{\partial r}$.

For the same conditions

$$\alpha \left(\frac{\partial^2 T}{\partial r^2} + \frac{2}{r} \frac{\partial T}{\partial r} \right) \approx 8 \times 10^{10}$$

and

$$\frac{\partial T}{\partial r} \cdot \frac{\partial \alpha}{\partial r} \approx 7 \times 10^{4}$$

justifying the assumption that $\frac{\partial T}{\partial r} \cdot \frac{\partial \alpha}{\partial r}$ can be neglected.

APPENDIX C

VARIATION OF A_1 AND B_1 WITH Re

A power series of the form

$$b_o + b_1.Re + b_2.Re^2 + b_3.Re^3 + b_4.Re^4$$

was fitted to the tabulated values of A_1 and B_1 vs Re (12) range $10 \leq Re \leq 100$.

The solution was gained by use of an IBM 7040 routine called MLTREG in the MILIS*library to give the following results

$$A_1 = -4.497 - 2.895 \times 10^{-4}.Re + 2.214 \times 10^{-4}.Re^2 - 2.96 \times 10^{-9}.Re^4 \qquad (C\text{-}1)$$

with std. error of estimate (σ) = 5.46×10^{-4};multiple correlation coefficient = 1.000 (at the 95% level of significance)

$$B_1 = 2.930 \times 10^{-2} + 8.845 \times 10^{-2}.Re + 1.1 \times 10^{-4}.Re^2 - 2.669 \times 10^{-7}.Re^3 \qquad (C\text{-}2)$$

with std. error of estimate (σ) = 5.645×10^{-3};multiple correlation coefficient = 1.000 (at the 95% level of significance)

---

* MILIS - McMaster Internal Library and Information Sheets

APPENDIX D

FINITE DIFFERENCE APPROXIMATIONS

Taylor Series expansions about S(i,j) (where S is either concentration of temperature) can be written as:

$$S(i+1,j) = S(i,j) + \frac{\partial S}{\partial \Theta} \cdot \Delta\Theta \qquad \text{(D-1)}$$

to first order

or

$$S(i,j+1) = S(i,j) + \frac{\partial S}{\partial r} \cdot \Delta r + \frac{\partial^2 S}{\partial r^2} \cdot \frac{(\Delta r)^2}{2} \qquad \text{(D-2)}$$

$$S(i,j-1) = S(i,j) - \frac{\partial S}{\partial r} \cdot \partial r + \frac{\partial^2 S}{\partial r^2} \cdot \frac{(\Delta r)^2}{2} \qquad \text{(D-3)}$$

to second order

from (D-1)

$$\frac{\partial S}{\partial \Theta}\Big|_{(i,j)} = \frac{S(i,j+1) - S(i,j-1)}{\Delta\,\Theta} \qquad \text{(D-4)}$$

and from (D-2) and (D-3)

$$\frac{\partial S}{\partial r}\Big|_{(i,j)} = \frac{S(i,j+1) - S(i,j-1)}{2.\Delta r} \qquad \text{(D-5)}$$

$$\frac{\partial^2 S}{\partial r^2}_{(i,j)} = \frac{S(i,j+1) - 2.S(i,j) + S(i,j-1)}{(\Delta r)^2} \qquad \text{(D-6)}$$

APPENDIX E

DEVELOPMENT OF FINITE DIFFERENCE EQUATIONS

Starting with

$$V_r \frac{\partial T}{\partial r} + \frac{V_\Theta}{r} \frac{\partial T}{\partial \Theta} = \frac{2}{Pe_H} \left(\frac{\partial^2 T}{\partial r^2} + \frac{1}{r} \frac{\partial T}{\partial r} \right) \qquad (T\text{-}4)$$

and substituting the finite difference approximations of Appendix D for the partial derivatives leads to (upon rearrangement):

$$T(i+1,j) \left[\frac{V_r}{4.\Delta r} - \frac{1}{Pe_H(\Delta r)^2} - \frac{1}{Pe_H.r.\Delta r} \right]$$

$$+ T(i-1,j) \left[- \frac{V_r}{4\Delta r} - \frac{1}{Pe_H(\Delta r)^2} + \frac{1}{Pe_H.r.\Delta r} \right]$$

$$+ T(i+1,j+1) \left[\frac{V_r}{4\Delta r} - \frac{1}{Pe_H(\Delta r)^2} - \frac{1}{Pe_H.r.\Delta r} \right]$$

$$+ T(i-1,j+1) \left[- \frac{V_r}{4\cdot\Delta r} - \frac{1}{Pe_H(\Delta r)^2} + \frac{1}{Pe.r.\Delta r} \right]$$

$$+ T(i,j+1) \left[\frac{V_\Theta}{r\cdot\Delta\Theta} + \frac{2}{Pe(\Delta r)^2} \right]$$

$$+ T(i,j) \left[- \frac{V_\Theta}{r\cdot\Delta\Theta} + \frac{2}{Pe(\Delta r)^2} \right] = 0$$

which, by further rearrangement, and the hindsight definition of

$$a = \frac{\Delta\Theta.r}{Pe_H.(\Delta r)^2 V_\Theta}$$

$$b = \frac{\Delta\,\Theta}{Pe_H.(\Delta r).V_\Theta} - \frac{\Delta\Theta.r.V_r}{4(\Delta r).V\Theta}$$

leads to the final equation

$$(a+b)\,(T(i+1,j+1) + T(i,j+1)) + (a-b)\,(T(i+1,j-1) + T\,(i,j-1)) - T(i,j) = (2a+1)\,T\,(i+1,j) \qquad (T\text{-}5)$$

and the analagous

$$(a+b)\,(C(i+1,j+1) + C(i,j+1)) + (a-b)\,(C(i+1,j-1) + C\,(i,j-1)) - C(i,j) = (2a+1)\,C\,(i+1,j) \qquad (T\text{-}7)$$

with a, b defined for Pe_M.

APPENDIX F

Hamielec, Lu and McLean present a formula for calculation of fluxes based on two arbitrary temperatures, a film temperature T_f and an "effective" temperature, T_E.

$$\text{Flux} = \frac{\overline{N}_{Sh_f} \cdot D_{AB_f} \cdot p}{D_p \cdot RT_E} \cdot X_A \text{ (bulk)}$$

and if $T_f = T_E$ this becomes

$$\text{Flux} = \frac{\overline{N}_{Sh_f} \cdot D_{AB_f} \cdot p}{D_p \cdot RT_f} \cdot X_A \text{ (bulk)}$$

They use the Ranz-Marshall correlation

$$\overline{N}_{Sh_f} = 2.0 + 0.6 \cdot Sc_f^{1/3} Re_f^{1/2}$$

for the Sherwood number.

APPENDIX G

The Reynolds number is defined as

$$Re = \frac{D_p \cdot \rho \cdot U}{\mu} = \frac{D_p U}{\nu}$$

where $\nu = \frac{\mu}{\rho}$ = kinematic necessity

Thus, if a calculation is done for a particular Reynolds number it only requires that the product of velocity and diameter be constant. Thus a small drop at high velocity can have the same Re as a large drop at low velocity, and so can have the same Sherwood number. This allows an entire body of solutions to be incorporated in one calculation, introduction of drop size coming later.

APPENDIX H

F_1 = correct finite-difference flux

F_2 = "isothermal" or T_f flux

$$F_1 = A.F_2 \cdot \frac{T_f}{T_b} \cdot \left(\frac{T_d}{T_f} \right)^B$$

but $T_f = \dfrac{T_d + T_b}{2}$

$$\frac{F_1}{F_2} = A \cdot \left(\frac{T_d + T_b}{2\,T_b} \right) \left(\frac{2\,T_d}{T_d + T_b} \right)^B$$

$$= A. \left(\frac{Td/Tb + 1}{2} \right) \left(\frac{2\,Td/Tb}{T_d/T_b + 1} \right)^B$$

but Td/Tb = X

$$\frac{F_1}{F_2} = A \left(\frac{X + 1}{2} \right) \left(\frac{2X}{X + 1} \right)^B$$

$$= A\,X^B \left(\frac{2}{X + 1} \right)^{B-1}$$

i.e. $$\frac{F_1}{F_2} \left(\frac{2}{X + 1} \right) = A \left(\frac{2X}{X + 1} \right)^B$$

or Flux ("true") = Flux (T_f) . A . $\left(\dfrac{X + 1}{2}\right)$. $\left(\dfrac{2X}{X + 1}\right)^B$

APPENDIX I

HEAT TRANSFER FROM A FALLING DROP

From the Nusselt number data presented in Appendix J, it is possible to calculate the total heat loss of a falling drop and so to predict (exclusive of any heat of reaction) the temperature at any time.

The relationship is strictly empirical, deriving from calculations of Reynolds number as a function of time for various drop diameters and Nusselt number as a function of Reynolds number. This relationship is given by

$$\text{Total heat loss to time } t = \int_0^t (\text{instantaneous convection loss})\, dt + \int_0^t (\text{instantaneous radiation loss})\, dt$$

$$\text{i.e. } \int_0^t \rho_L C_p \frac{\pi d^3}{6} \frac{\partial T}{\partial t} = \int_0^t \pi d\, (T-T_\infty)\, (6.8 + 40.9 \times dxt)\, dt + \int_0^t 1.192 \times 10^{-12}\, T^4\, dt$$

where K_s is the thermal conductivity of the gas at drop surface (temperature T); d is drop diameter in cm.

Assuming x, the fall distance can be represented by $\frac{gt^2}{2}$, the temperature can be calculated as a function of fall distance and these results are summarized in Table (I-1). Calculations were done for O_2 - N_2

gas mixtures with similar heat capacities (e.g. CO_2 - N_2).

Inclusion of heat of reaction would simply add a negative source term to the total heat loss expression used. Since this varies so much from reaction to reaction, it was not included here.

TABLE T-1

Drop diameter
1.00000E-01 (cm)

Time (sec)	Temperature (°C)	X (cm.)
-0.	1.80000E 03	0.
5.00000E-02	1.33157E 03	1.22500E 00
1.00000E-01	1.00277E 03	4.90000E 00
1.50000E-01	7.77102E 02	1.10250E 01
2.00000E-01	6.25261E 02	1.96000E 01
2.50000E-01	5.24901E 02	3.06250E 01
3.00000E-01	4.59638E 02	4.41000E 01
3.50000E-01	4.17835E 02	6.00250E 01
4.00000E-01	3.91440E 02	7.84000E 01
4.50000E-01	3.75000E 02	9.92250E 01
5.00000E-01	3.64897E 02	1.22500E 02
5.50000E-01	3.58768E 02	1.48225E 02
6.00000E-01	3.55098E 02	1.76400E 02
6.50000E-01	3.52928E 02	2.07025E 02
6.00000E-01	3.51662E 02	2.40100E 02
7.50000E-01	3.50932E 02	2.75625E 02
8.00000E-01	3.50516E 02	3.13600E 02
8.50000E-01	3.50282E 02	3.54025E 02
9.00000E-01	3.50153E 02	3.96900E 02
9.50000E-01	3.50081E 02	4.42225E 02
1.00000E 00	3.50043E 02	4.90000E 02
1.05000E 00	3.50022E 02	5.40225E 02

TABLE T-1 (continued)

Drop diameter
2.00000E-01

Time (sec)	Temperature	X
-0.	1.80000E 03	0.
5.00000E-02	1.66426E 03	1.22500E 00
1.00000E-01	1.53378E 03	4.90000E 00
1.50000E-01	1.40953E 03	1.10250E 01
2.00000E-01	1.29233E 03	1.96000E 01
2.50000E-01	1.18278E 03	3.06250E 01
3.00000E-01	1.08127E 03	4.41000E 01
3.50000E-01	9.88043E 02	6.00250E 01
4.00000E-01	9.03152E 02	7.84000E 01
4.50000E-01	8.26499E 02	9.92250E 01
5.00000E-01	7.57857E 02	1.22500E 02
5.50000E-01	6.96886E 02	1.48225E 02
6.00000E-01	6.43162E 02	1.76400E 02
6.50000E-01	5.96194E 02	2.07025E 02
7.00000E-01	5.55450E 02	2.40100E 02
7.50000E-01	5.20375E 02	2.74625E 02
8.00000E-01	4.90405E 02	3.13600E 02
8.50000E-01	4.64987E 02	3.54025E 02
9.00000E-01	4.43586E 02	3.96900E 02
9.50000E-01	4.25697E 02	4.42225E 02
1.00000E 00	4.10851E 02	4.90000E 02
1.05000E 00	3.98615E 02	5.40225E 02

TABLE T-1 (continued)

Drop diameter
3.00000E-01

Time (sec)	Temperature	X
-0.	1.80000E 03	0.
5.00000E-02	1.73727E 03	1.22500E 00
1.00000E-01	1.67202E 03	4.90000E 00
1.50000E-01	1.60486E 03	1.10250E 01
2.00000E-01	1.53637E 03	1.96000E 01
2.50000E-01	1.46712E 03	3.06250E 01
3.00000E-01	1.39768E 03	4.41000E 01
3.50000E-01	1.32858E 03	6.00250E 01
4.00000E-01	1.26032E 03	7.84000E 01
4.50000E-01	1.19336E 03	9.92250E 01
5.00000E-01	1.12812E 03	1.22500E 02
5.50000E-01	1.06497E 03	1.48225E 02
6.00000E-01	1.00423E 03	1.76400E 02
6.50000E-01	9.46175E 02	2.07025E 02
7.00000E-01	8.91016E 02	2.40100E 02
7.50000E-01	8.38919E 02	2.75625E 02
8.00000E-01	7.90002E 02	3.13600E 02
8.50000E-01	7.44330E 02	3.54025E 02
9.00000E-01	7.01927E 02	3.96900E 02
9.50000E-01	6.62777E 02	4.42225E 02
1.00000E 00	6.26825E 02	4.90000E 02
1.05000E 00	5.93987E 02	5.40225E 02

TABLE T-1 (continued)

Drop diameter
4.00000E-01

Time (sec)	Temperature	X
-0.	1.80000E 03	0.
5.00000E-02	1.76395E 03	1.22500E 00
1.00000E-01	1.72479E 03	4.90000E 00
1.50000E-01	1.68281E 03	1.10250E 01
2.00000E-01	1.63834E 03	1.96000E 01
2.50000E-01	1.59168E 03	3.06250E 01
3.00000E-01	1.54318E 03	4.41000E 01
3.50000E-01	1.49316E 03	6.00250E 01
4.00000E-01	1.44198E 03	7.84000E 01
4.50000E-01	1.38996E 03	9.92250E 01
5.00000E-01	1.33744E 03	1.22500E 02
5.50000E-01	1.28474E 03	1.48225E 02
6.00000E-01	1.23217E 03	1.76400E 02
6.50000E-01	1.18002E 03	2.07025E 02
7.00000E-01	1.12857E 03	2.40100E 02
7.50000E-01	1.07807E 03	2.75625E 02
8.00000E-01	1.02875E 03	3.13600E 02
8.50000E-01	9.80815E 02	3.54025E 02
9.00000E-01	9.34458E 02	3.96900E 02
9.50000E-01	8.89830E 02	4.42225E 02
1.00000E 00	8.47063E 02	4.90000E 02
1.05000E 00	8.06263E 02	5.40225E 02

TABLE T-1 (continued)

Drop diameter
5.00000E-01

Time (sec)	Temperature	X
-0.	1.80000E 03	0.
5.00000E-02	1.77659E 03	1.22500E 00
1.00000E-01	1.75032E 03	4.90000E 00
1.50000E-01	1.72134E 03	1.10250E 01
2.00000E-01	1.68985E 03	1.96000E 01
2.50000E-01	1.65602E 03	3.06250E 01
3.00000E-01	1.62007E 03	4.41000E 01
3.50000E-01	1.58220E 03	6.00250E 01
4.00000E-01	1.54265E 03	7.84000E 01
4.50000E-01	1.50163E 03	9.92250E 01
5.00000E-01	1.45938E 03	1.22500E 02
5.50000E-01	1.41613E 03	1.48225E 02
6.00000E-01	1.37211E 03	1.76400E 02
6.50000E-01	1.32755E 03	2.07025E 02
7.00000E-01	1.28268E 03	2.40100E 02
7.50000E-01	1.23772E 03	2.75625E 02
8.00000E-01	1.19287E 03	3.13600E 02
8.50000E-01	1.14833E 03	3.54025E 02
9.00000E-01	1.10430E 03	3.96900E 02
9.50000E-01	1.06095E 03	4.42225E 02
1.00000E 00	1.01845E 03	4.90000E 02
1.05000E 00	9.76937E 02	5.40225E 02

APPENDIX J

Raw Data

$N_2 - O_2$

X_{O_2}	Re	$\overline{M}_{N_u}$	Flux * radius (cmxcal/sec)	$\overline{N}_{Sh}$	Flux * radius (moles/cm/sec)
0.2	10	8.5253	1.8478	8.0708	1.8379×10^{-4}
		8.5202	1.4959	8.0885	1.5366
		8.5148	1.1033	8.1097	1.2429
		8.5096	8.1376×10^{-1}	8.1349	9.7739×10^{-5}
		8.5039	5.7223	8.1650	7.4068
		8.4978	3.7450	8.2013	5.3359
		8.4914	2.1716	8.2458	3.5718
		8.4847	9.7704×10^{-2}	8.3010	2.1284
		8.5663	6.6625×10^{-4}	7.8489	2.092×10^{-5}
		8.5578	6.1671	6.8673	1.90
		8.5488	5.6821	7.8930	1.76
		8.5391	5.2058	7.9276	1.62
		8.5288	9.7364	7.9731	1.48
		8.5177	4.2715	8.0324	1.33
		8.5057	3.8079	8.1098	1.17
		8.4930	3.3412	8.2125	1.02

Raw Data

$N_2 - O_2$

X_{Oxid}	Re	Td	$\overline{N}_{Nu}$	Flux x radius	$\overline{N}_{Sh}$	Flux x radius
0.2	50	2000	15.4671	3.3518	14.5279	3.3493×10^{-4}
		1800	15.4546	2.6228	14.5627	2.7665
		1600	15.4444	2.0011	14.6042	2.2383
		1400	15.4338	2.4759	14.6537	1.7606
		1200	15.4227	1.0378	14.7128	1.3346
		1000	15.4109	6.7916×10^{-1}	14.7842	9.6189×10^{-5}
		800	15.3983	3.9381	14.8719	6.4420
		600	15.3852	1.7717	14.9822	3.8412
		T_f				
		1175	15.5413	1.2087×10^{-3}	14.1131	3.68
		1075	15.5252	1.1188	14.1484	3.42
		975	15.5078	1.0308	14.1979	3.17
		875	15.4894	9.4430×10^{-4}	14.2695	2.91
		775	15.4696	8.5910	14.3520	2.66
		675	15.4482	7.7470	14.4662	2.39
		575	15.4254	6..0057	14.6155	2.12
		475	15.4009	6.0588	14.8139	1.84

Raw Data

N_2 - O_2

X_{Oxid}	Re	Td	$\overline{N}_{Nu}$	Flux x radius	$\overline{N}_{Sh}$	Flux x radius
0.2	100	2000	23.7318	5.1438	22.2845	5.1299×10^{-4}
		1800	23.7161	4.0248	22.3407	4.2441
		1600	23.6999	3.0708	22.4081	3.4343
		1400	23.6827	2.2647	22.4888	2.7020
		1200	23.6646	1.4924	22.5857	2.0488
		1000	23.6455	1.0421	22.7033	1.4771
		800	22.6253	6.0421×10^{-1}	22.8982	9.8971×10^{-5}
		600	23.6037	2.7180	23.0313	5.9049
		T_f				
		1175	23.8532	1.8552×10^{-3}	21.6269	5.64
		1075	23.8275	1.7171	21.6851	5.24
		975	23.7997	1.5819	21.7645	4.86
		875	23.7699	1.4491	21.8726	4.47
		775	23.7381	1.3183	22.0148	4.08
		675	23.7091	1.1887	22.2002	3.67
		575	23.6675	1.0595	22.4430	3.25
		475	23.6282	9.2954×10^{-4}	22.7654	2.82

Raw Data

$N_2 - O_2$

X_{Oxid}	Re	Td	$\overline{N}_{Nu}$	Flux x radius	$\overline{N}_{Sh}$	Flux x radius
0.4	10	2000	8.6013	1.8427	8.1559	3.2597×10^{-4}
		1800	8.5966	1.4546	8.1748	3.1060
		1600	8.5914	1.1180	8.1972	2.5126
		1400	8.5855	8.2940×10^{-1}	8.2236	1.9761
		1200	8.5795	5.8581	8.2551	1.4977
		1000	8.5731	3.8451	8.2929	1.0791
		800	8.5660	2.2327	8.3390	7.2249×10^{-5}
		600	8.5584	1.0042	8.3967	4.3056
		T_f				
		1175	8.6437	6.8244×10^{-4}	7.9234	4.14
		1075	8.6358	6.3275	7.9492	3.85
		975	8.6270	5.8371	7.9724	3.56
		875	8.6173	5.3522	8.0096	3.274
		775	8.6065	4.8714	8.0577	2.98
		675	8.5950	4.3731	8.1196	2.69
		575	8.5819	3.9140	8.2000	2.38
		475	8.5680	3.4309	8.3059	2.06

Raw Data

N_2 - O_2

X_{Oxid}	Re	Td	$\overline{N}_{Nu}$	Flux x radius	$\overline{N}_{Sh}$	Flux x radius
0.4	50	2000	15.6098	3.3442	14.6915	6.7639×10^{-4}
		1800	15.6003	2.6396	14.7287	5.5960
		1600	15.5902	2.0287	14.7727	4.5282
		1400	15.5793	1.5050	14.8247	3.5623
		1200	15.5675	1.0629	14.8866	2.7008
		1000	15.5548	6.9764×10^{-1}	14.9610	1.9468
		800	15.5410	4.0507	15.0520	1.3040
		600	15.5266	1.8218	15.1662	7.7768×10^{-5}
		T_f				
		1175	15.6888	1.2387×10^{-3}	14.2562	7.45
		1075	15.6738	1.1484	14.2963	6.92
		975	15.6571	1.0594	14.3502	6.41
		875	15.6386	9.7132×10^{-4}	14.4223	5.90
		775	15.6182	8.8402	14.5149	5.38
		675	15.5958	7.9713	14.6345	4.84
		575	14.5712	7.1017	14.7897	4.29
		475	15.5441	6.2243	14.9945	3.72

Raw Data

N_2 - O_2

X_{Oxid}	Re	Td	$\overline{N}_{Nu}$	Flux x radius	$\overline{N}_{Sh}$	Flux x radius
0.4	100	2000	23.9697	5.1342	22.5503	1.0382×10^{-3}
		1800	23.9476	4.0524	22.6105	8.4706×10^{-4}
		1600	23.9333	3.1144	22.6819	6.9526
		1400	23.9156	2.3104	22.7669	5.4708
		1200	23.8965	1.6317	22.8684	4.1489
		1000	23.8763	1.0709	22.9910	2.9917
		800	23.8539	6.2174×10^{-1}	23.1414	2.0048
		600	23.8303	2.7760	23.3310	1.1963
		T_f				
		1175	24.0897	1.9020×10^{-3}	21.8592	1.138×10^{-4}
		1075	24.0655	1.7633	21.9243	1.06
		975	24.0388	1.6265	22.0126	9.84×10^{-5}
		875	24.0091	1.4912	22.1289	9.05
		775	23.9761	1.3571	22.2795	8.25
		675	23.9402	1.2236	22.4738	7.43
		575	23.9010	1.0901	22.7261	6.59
		475	23.8577	9.5533×10^{-4}	23.0594	5.71

Raw Data

N_2 - O_2

X_{Oxid}	Re	Td	$\overline{N}_{Nu}$	Flux x radius	$\overline{N}_{Sh}$	Flux x radius
0.6	10	2000	8.6762	1.8368	8.2395	5.6901×10^{-4}
		1800	8.6714	1.4627	8.2596	4.7072
		1600	8.6657	1.1324	8.2832	3.8085
		1400	8.6597	8.4496×10^{-1}	8.3109	2.9956
		1200	8.6536	5.9941	8.3437	2.2707
		1000	8.6465	3.9456	8.3830	1.6362
		800	8.6388	2.2942	8.4307	1.0956
		600	8.6303	1.0316	8.4903	6.5309×10^{-5}
		T_f				
		1175	8.7195	6.9868×10^{-4}	7.9963	6.25×10^{-5}
		1075	8.7121	6.4886	8.0196	5.82
		975	8.7035	5.9931	8.0504	5.40
		875	8.6938	5.4998	8.0901	4.96
		775	8.6827	5.0078	8.1407	4.55
		675	8.6702	4.5156	8.2054	4.07
		575	8.6565	4.0214	8.2887	3.60
		475	8.6409	3.5214	8.3978	3.12

Raw Data

N_2 - O_2

X_{Oxid}	Re	Td	$\overline{N}_{Nu}$	Flux x radius	$\overline{N}_{Sh}$	Flux x radius
0.4	50	2000	15.7521	3.3348	14.8524	1.0257×10^{-3}
		1800	15.7429	2.6555	14.8921	8.4872×10^{-4}
		1600	15.7325	2.0558	14.9385	6.8685
		1400	15.7211	1.5340	14.9931	5.4042
		1200	15.7087	1.0881	15.0578	4.0978
		1000	15.6952	7.1622×10^{-1}	15.1352	2.9542
		800	15.6805	4.1643	15.2296	1.9791
		600	15.6692	1.8723	15.3477	1.1805
		T_f				
		1175	15.8334	1.2687×10^{-3}	14.3967	11.2×10^{-5}
		1075	15.8193	1.1782	14.4417	10.5
		975	15.8029	1.0882	14.5009	9.72
		875	15.7843	9.9853×10^{-4}	14.5774	8.94
		775	15.7633	9.0915	14.6753	8.75
		675	15.7396	8.1975	14.8002	7.34
		575	15.7133	7.2997	14.9612	6.51
		475	15.6838	6.3915	15.1726	5.64

Raw Data

N_2 - O_2

X_{Oxid}	Re	Td	$\overline{N}_{Nu}$	Flux x radius	$\overline{N}_{Sh}$	Flux x radius
0.6	100	2000	24.1925	5.1217	22.8117	1.5754×10^{-3}
		1800	24.1778	4.0783	22.8759	1.3037
		1600	24.1612	3.1572	22.9515	1.0553
		1400	24.1431	2.3557	23.0408	8.3045×10^{-4}
		1200	24.1231	1.6709	23.1469	6.2992
		1000	24.1010	1.0998	23.2745	4.5428
		800	24.0771	6.3942×10^{-1}	23.4305	3.0498
		600	24.0506	2.8747	23.6265	1.8173
		T_f				
		1175	24.3217	1.9489×10^{-3}	22.0874	17.25×10^{-5}
		1075	24.2990	1.8097	22.1604	16.1
		975	24.2726	1.1714	22.2567	14.9
		875	24.2428	1.5336	22.3811	13.7
		775	24.2091	1.3963	22.5401	12.5
		675	24.1712	1.2589	22.7433	11.3
		575	24.1289	1.1209	23.0052	10.0
		475	24.0816	9.8137×10^{-4}	23.3492	8.68

Raw Data

N_2 - O_2

X_{Oxid}	Re	Td	$\overline{N}_{Nu}$	Flux x radius	$\overline{N}_{Sh}$	Flux x radius
0.8	10	2000	8.7491	1.8299	8.3216	7.6625×10^{-4}
		1800	8.7442	1.4072	8.3429	6.3396
		1600	8.7388	1.1465	8.3678	5.1298
		1400	8.7327	8.6046×10^{-1}	8.3968	4.0354
		1200	8.7257	6.1300	8.4309	3.0592
		1000	8.7183	4.0467	8.4716	2.2047
		800	8.7100	2.3562	8.5210	1.4764
		600	8.7010	1.0593	8.5825	8.8017×10^{-5}
		T_f				
		1175	8.7941	7.1499×10^{-4}	8.0679	8.40×10^{-5}
		1075	8.7872	6.6507	8.0937	7.84
		975	8.7787	6.1502	8.1270	7.26
		875	8.7687	5.6485	8.1692	6.68
		775	8.7574	5.1454	8.2225	6.09
		675	8.7443	4.6396	8.2899	5.48
		575	8.7295	4.1299	8.3760	4.86
		475	8.7125	8.6129	8.4883	4.21

Raw Data

$N_2 - O_2$

X_{Oxid}	Re	Td	$\overline{N}_{Nu}$	Flux x radius	$\overline{N}_{Sh}$	Flux x radius
0.8	50	2000	15.8914	3.3237	15.0108	1.3822×10^{-3}
		1800	15.8822	2.6703	15.0528	1.1438
		1600	15.8717	2.0823	15.1017	9.2581×10^{-4}
		1400	15.8599	1.5627	15.1590	7.2853
		1200	15.8466	1.1133	15.2264	5.5250
		1000	15.8321	7.3487×10^{-1}	15.3069	3.9836
		800	15.8161	4.2786	15.4047	2.6691
		600	15.7982	1.9233	15.5268	1.5923
		T_f				
		1175	15.9754	1.2989×10^{-3}	14.5347	15.1×10^{-5}
		1075	15.9618	1.2081	14.5845	14.1
		975	15.9461	1.1172	14.6987	13.1
		875	15.9273	1.0260	14.7302	12.0
		775	15.9057	9.3453×10^{-4}	14.8336	11.0
		675	15.8808	8.4262	14.9636	9.90
		575	15.8522	7.4996	15.1304	8.77
		475	15.8201	6.5603	15.3483	7.61

Raw Data

N_2 - O_2

X_{Oxid}	Re	Td	$\overline{N}_{Nu}$	Flux x radius	$\overline{N}_{Sh}$	Flux x radius
0.8	100	2000	24.4156	5.1066	23.0681	2.1242×10^{-3}
		1800	24.4010	4.1025	23.1373	1.7582
		1600	24.3841	3.1991	23.2171	1.4233
		1400	24.3651	2.4008	23.3107	1.1203
		1200	24.3441	1.7102	23.4215	8.4986×10^{-4}
		1000	24.3208	1.1289	23.5541	6.1299
		800	24.2949	6.4723×10^{-1}	23.7157	4.1092
		600	24.2659	2.9541	23.9183	2.4529
		T_f				
		1175	24.5492	1.9959×10^{-3}	22.3116	2.32×10^{-5}
		1075	24.5275	1.8564	22.3925	2.17
		975	24.5019	1.7166	22.4968	2.01
		875	24.4721	1.5764	22.6294	1.85
		775	24.4372	1.4358	22.7969	1.69
		675	24.3973	1.2945	23.0091	1.52
		575	24.3518	1.1521	23.2806	1.35
		475	24.3001	1.0077	23.6353	1.17

Raw Data

N_2 - CO_2

X_{Oxid}	Re	Td	$\overline{N}_{Nu}$	Flux x radius	$\overline{N}_{Sh}$	Flux x radius
0.2	10	2000	8.7775	1.7800	8.6277	1.5072×10^{-4}
		1800				
		1600	8.7644	1.0849	8.6757	1.0090
		1400				
		1200	8.7479	5.6872×10^{-1}	8.7428	6.0184×10^{-5}
		1000				
		800				
		600	8.7166	9.6468×10^{-2}	8.9072	1.7330
		351	8.7001	2.6733×10^{-4}	9.0215	6.6048×10^{-6}
		T_f				
		1175	8.8344	6.6406×10^{-4}	8.3907	1.66×10^{-5}
		1075				
		975	8.8199	5.6670	8.4489	1.43
		875				
		775	8.7878	4.7126	8.5445	1.20
		675				
		575				
		475	8.7308	3.2843	8.8170	0.825

Raw Data

N_2 - CO_2

X_{Oxid}	Re	Td	$\overline{N}_{Nu}$	Flux x radius	$\overline{N}_{Sh}$	Flux x radius
0.2	100	2000	24.5028	4.9691	24.0368	4.1970×10^{-4}
		1800				
		1600	24.4628	3.0282	24.1911	2.8135
		1400				
		1200	24.4122	1.5871	24.4090	1.6803
		1000				
		800				
		600	24.3131	2.6909×10^{-1}	24.9500	4.8543×10^{-5}
		T_f				
		1175	24.6721	1.8545×10^{-3}	23.3271	4.610×10^{-5}
		1075				
		975	24.6121	1.5828	23.5092	3.985
		875				
		775	24.5294	1.3154	23.8132	3.344
		675				
		575				
		475	24.3560	9.1620×10^{-4}	24.6784	2.320

Raw Data

N_2 - CO_2

X_{Oxid}	Re	Td	$\overline{N}_{Nu}$	Flux x radius	$\overline{N}_{Sh}$	Flux x radius
0.80	10	2000	9.6580	1.5879	8.6635	6.0537×10^{-4}
		1800				
		1600	9.6433	1.0689	8.7201	4.0567
		1400				
		1200	9.6211	5.9103×10^{-1}	8.7927	2.4211
		1000				
		800				
		600	9.5720	9.9431×10^{-2}	8.9567	6.9705×10^{-5}
		T_f				
		1175	9.7301	6.9237×10^{-4}	8.2973	6.56×10^{-5}
		1075				
		975	9.7108	5.9653	8.3896	5.70
		875				
		775	9.6785	4.9419	8.5188	4.78
		675				
		575				
		475	9.5963	3.3282	8.8395	3.32

Raw Data

N_2 - CO_2

X_{Oxid}	Re	Td	$\overline{N}_{Nu}$	Flux x radius	$\overline{N}_{Sh}$	Flux x radius
0.8	100	2000	27.1966	4.4713	24.1483	1.6874×10^{-3}
		1800				
		1600	27.1492	3.0092	24.3320	1.1320
		1400				
		1200	27.0814	1.6636	24.5693	6.7653×10^{-4}
		1000				
		800				
		600	26.9306	2.7975×10^{-1}	25.1097	1.9541×10^{-4}
		T_f				
		1175	27.4112	1.9505×10^{-3}	23.0324	1.821×10^{-4}
		1075				
		975	27.3526	1.6803	23.3234	1.582
		875				
		775	27.2539	1.3916	23.7317	1.333
		675				
		575				
		475	27.0017	9.3648×10^{-4}	24.7502	0.9306

Raw Data

He - O_2

X_{Oxid}	Re	Td	$\overline{N}_{Nu}$	Flux x radius	$\overline{N}_{Sh}$	Flux x radius
0.2	10	2000	5.4572	4.1668	5.8732	5.4328×10^{-4}
		1800				
		1600	5.4479	2.7602	5.9232	3.6979
		1400				
		1200	5.4376	1.5850	5.9876	2.1826
		1000				
		800				
		600	5.4200	3.1596×10^{-1}	6.1339	6.3194×10^{-5}
		T_f				
		1175	5.4969	1.8633×10^{-3}	5.6920	5.957×10^{-5}
		1075				
		975	5.4809	1.6714	5.7614	5.172
		875				
		775	5.4621	1.4659	5.8549	4.354
		675				
		575				
		475	5.4283	1.1177	6.0782	3.025

Raw Data

He - O_2

X_{Oxid}	Re	Td	$\overline{N}_{Nu}$	Flux x radius	$\overline{N}_{Sh}$	Flux x radius
0.8	10	2000	7.7180	2.2775	5.8130	2.1509×10^{-3}
		1800				
		1600	7.6985	1.4595	5.8350	1.4374
		1400				
		1200	7.6747	8.0052×10^{-1}	5.8633	8.5491×10^{-4}
		1000				
		800				
		600	7.6306	1.4520	5.9264	2.4423
		T_f				
		1175	7.7983	9.4303×10^{-4}	5.5449	2.321×10^{-4}
		1075				
		975	7.7685	8.2218	5.5887	2.007

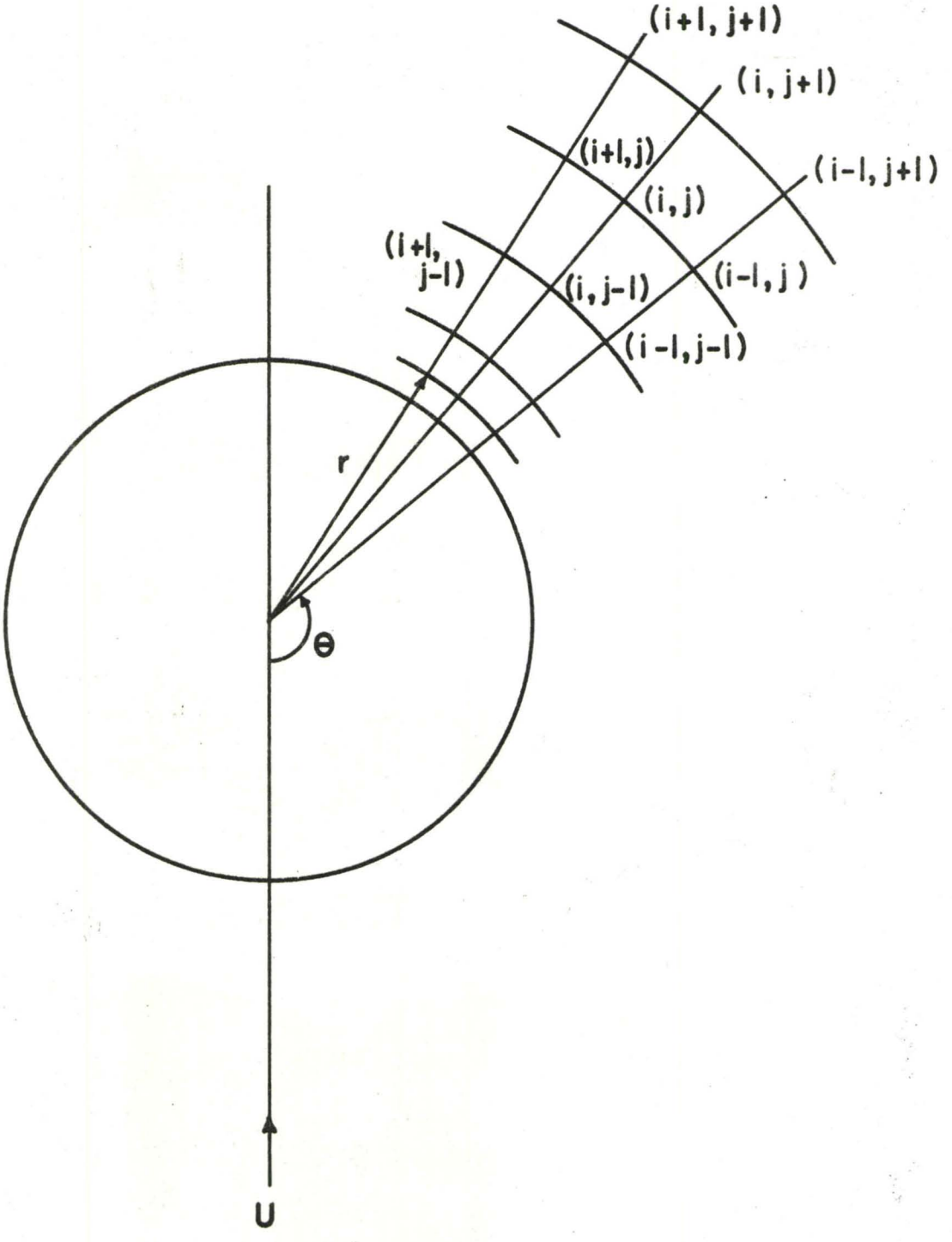

FINITE DIFFERENCE MESH

FIG. (T-1)

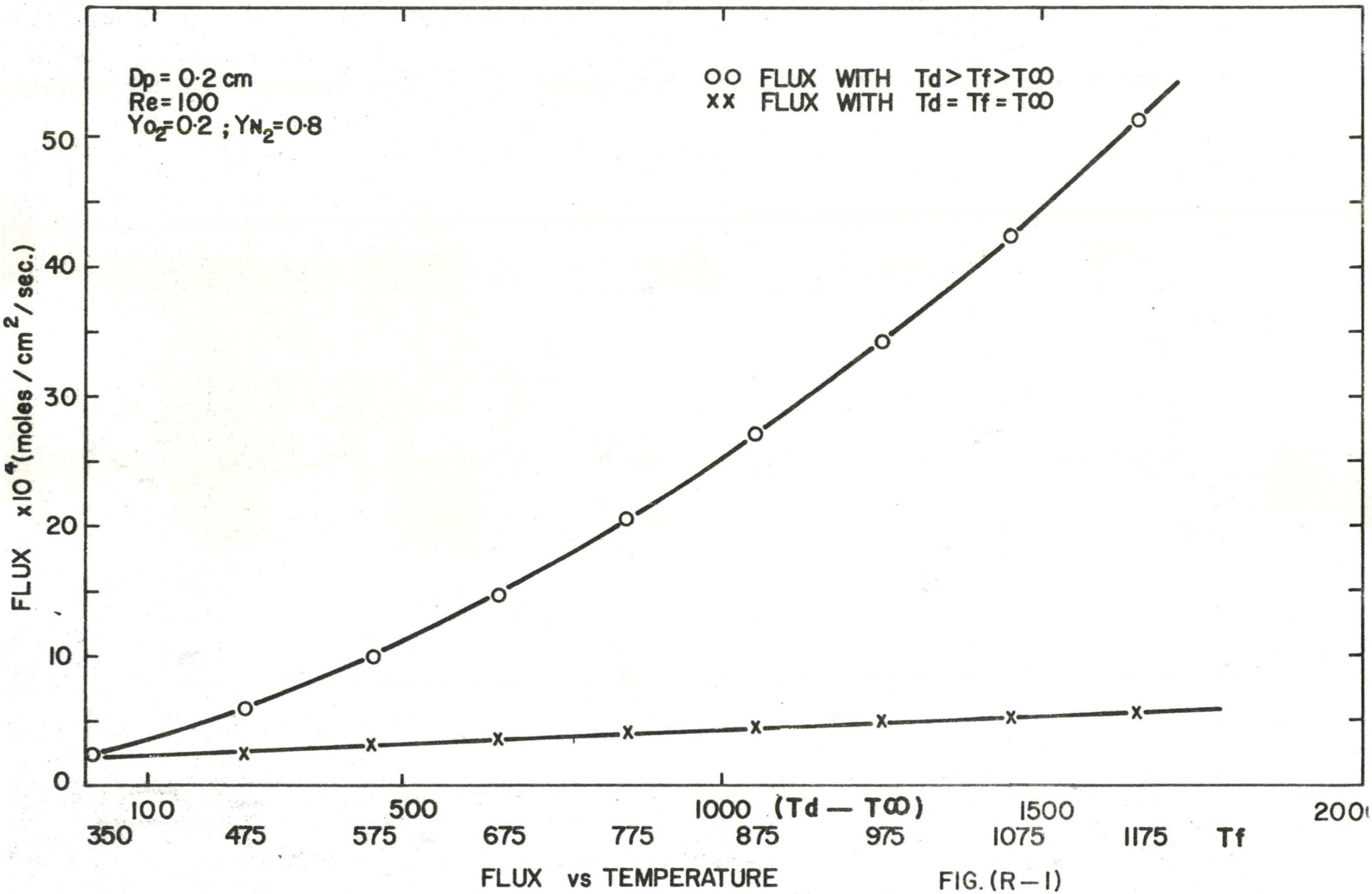

FLUX vs TEMPERATURE

FIG. (R—1)

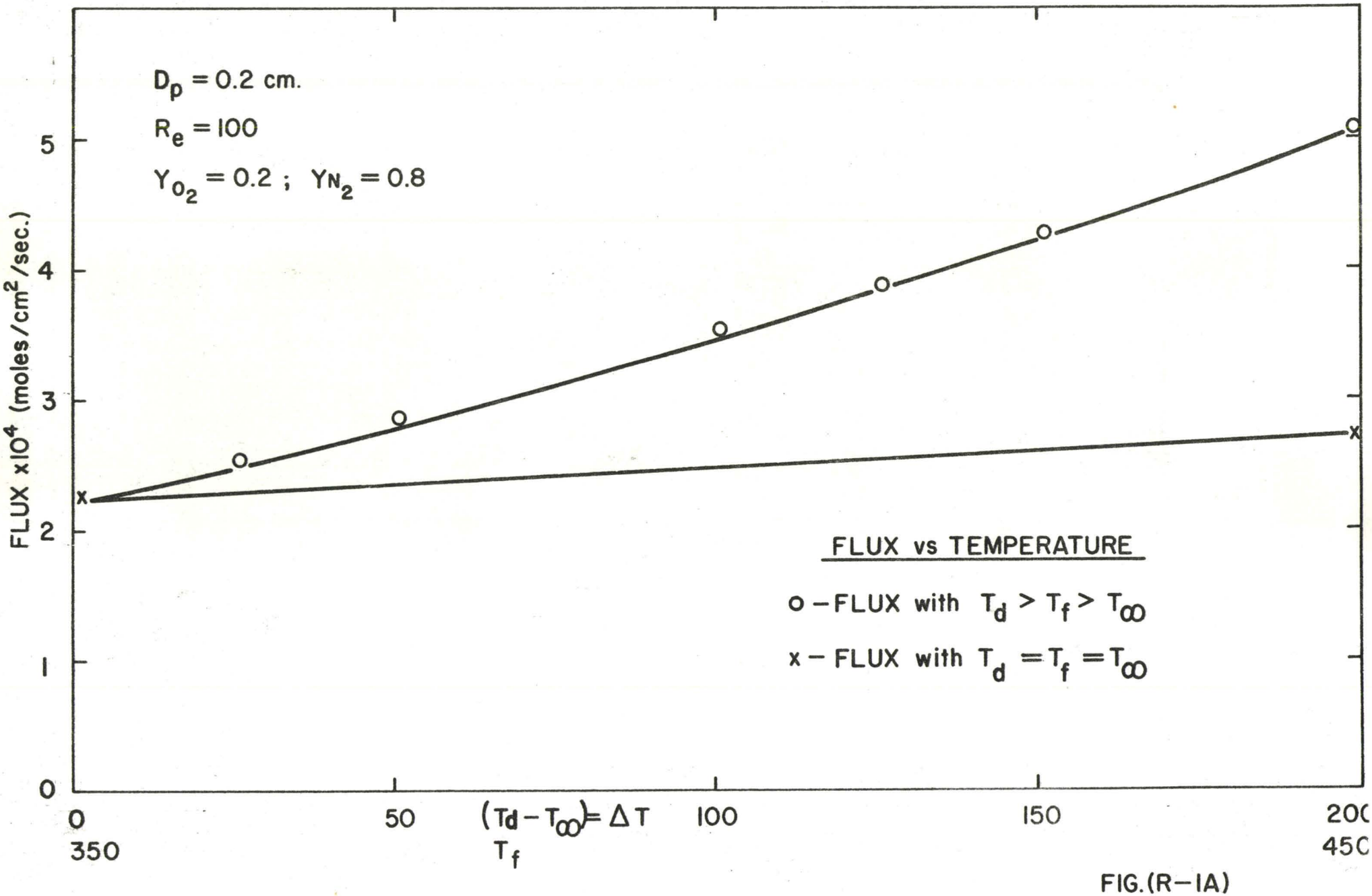
$D_p = 0.2$ cm.
$R_e = 100$
$Y_{O_2} = 0.2$; $Y_{N_2} = 0.8$
FLUX x10^4 (moles/cm^2/sec.)
0
1
2
3
4
5
FLUX vs TEMPERATURE
o – FLUX with $T_d > T_f > T_\infty$
x – FLUX with $T_d = T_f = T_\infty$
0
50
100
150
200
$(T_d - T_\infty) = \Delta T$
350
T_f
450

FIG.(R–1A)

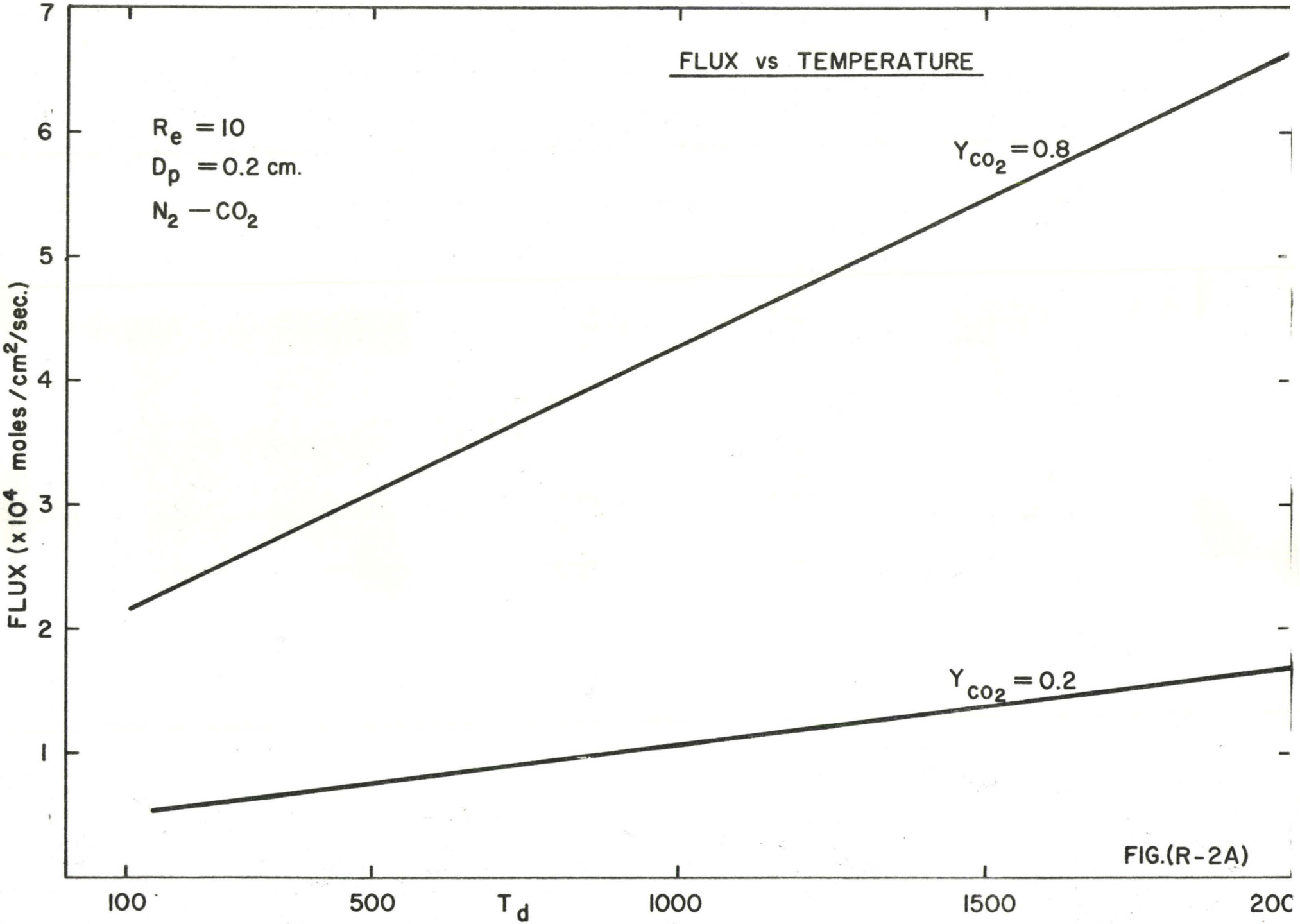
FLUX vs TEMPERATURE
$R_e = 10$
$D_p = 0.2$ cm.
$N_2 - CO_2$
$Y_{CO_2} = 0.8$
$Y_{CO_2} = 0.2$
FLUX ($\times 10^4$ moles / cm^2/sec.)
T_d
7
6
5
4
3
2
1
100
500
1000
1500
200

FIG.(R-2A)

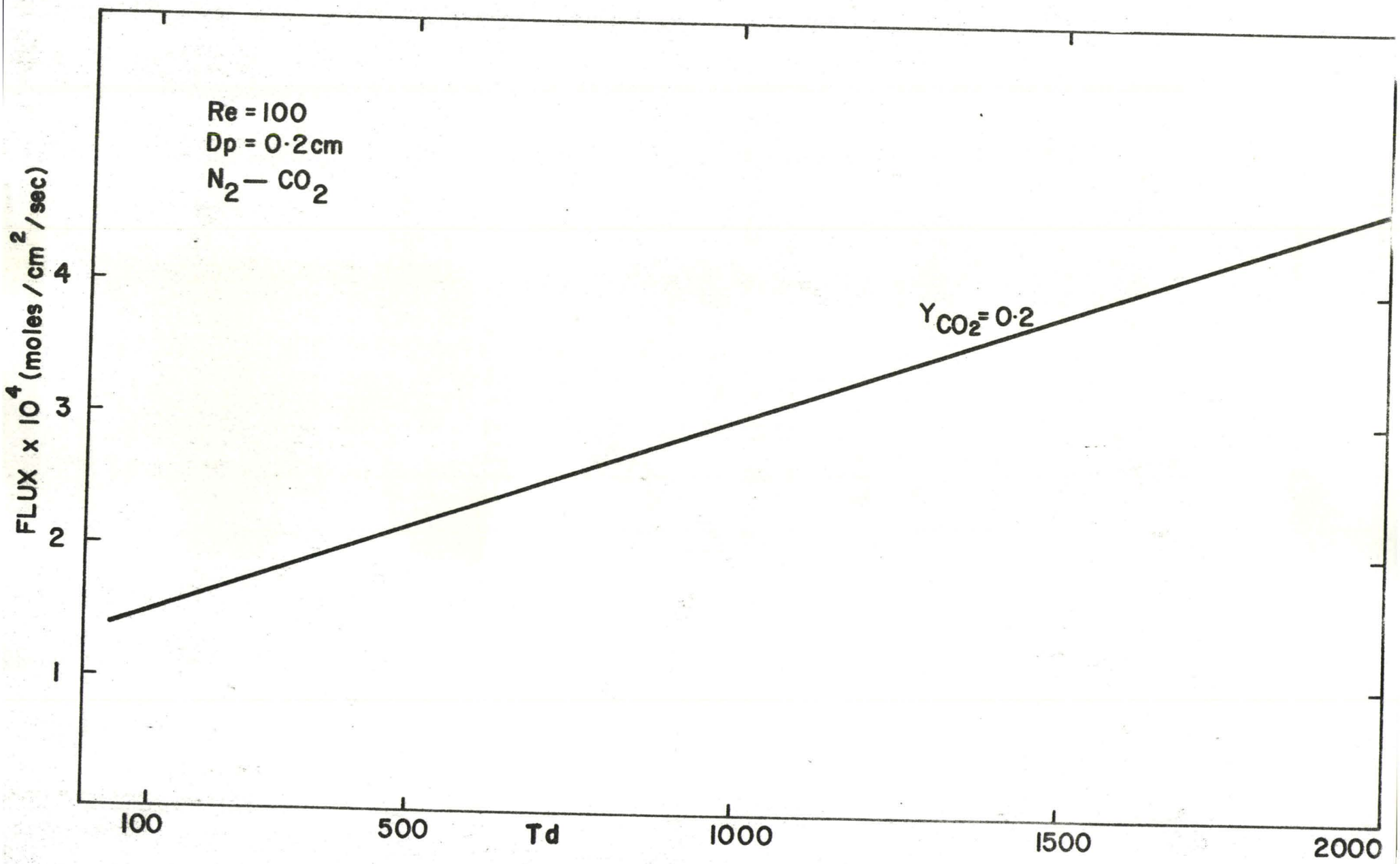

FLUX vs TEMPERATURE

FIG.(R–2B)

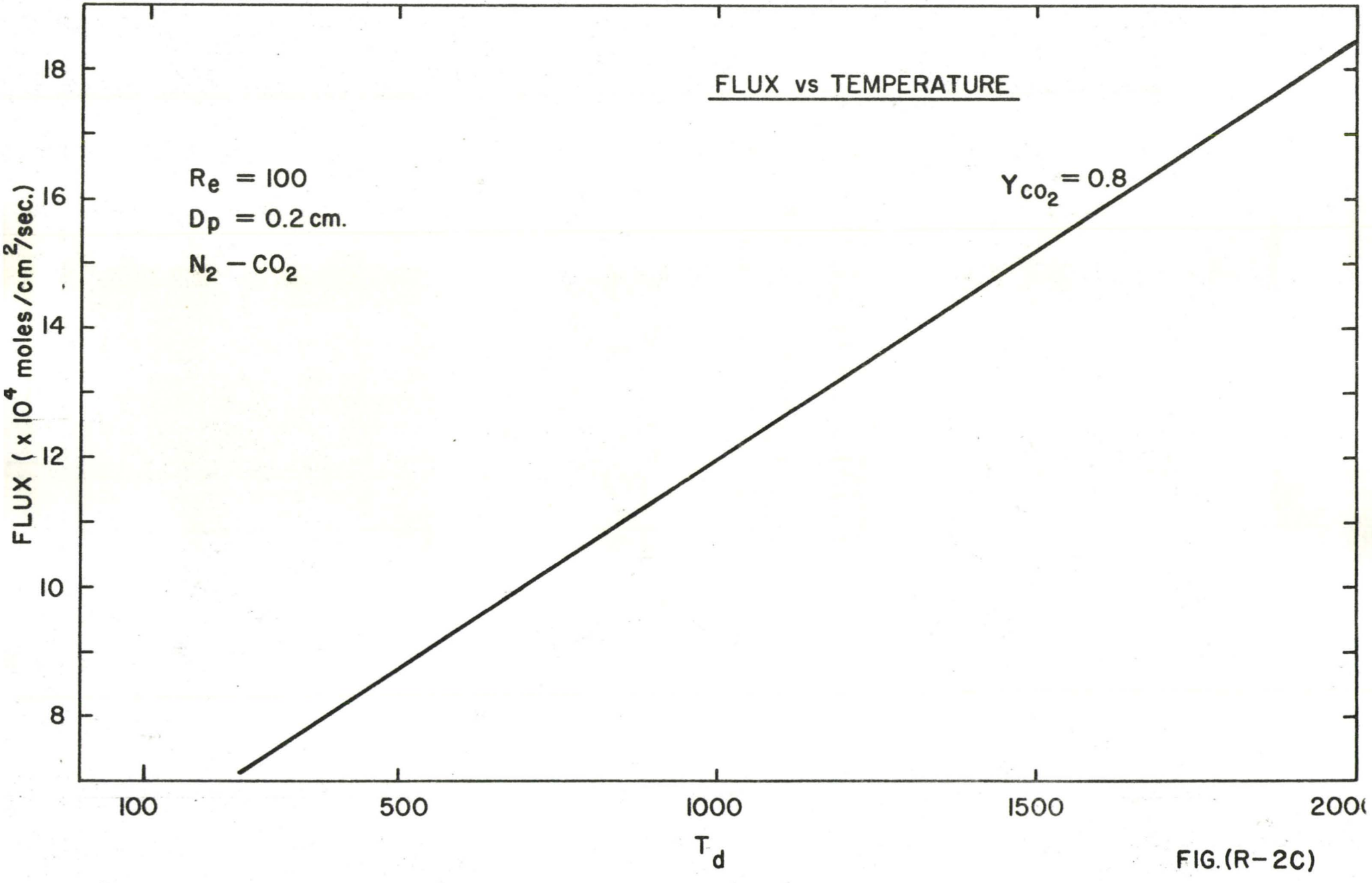
FLUX vs TEMPERATURE
$R_e = 100$
$D_p = 0.2$ cm.
$N_2 - CO_2$
$Y_{CO_2} = 0.8$
FLUX ($\times 10^4$ moles/cm^2/sec.)
18
16
14
12
10
8
100
500
1000
1500
200
T_d

FIG.(R-2C)

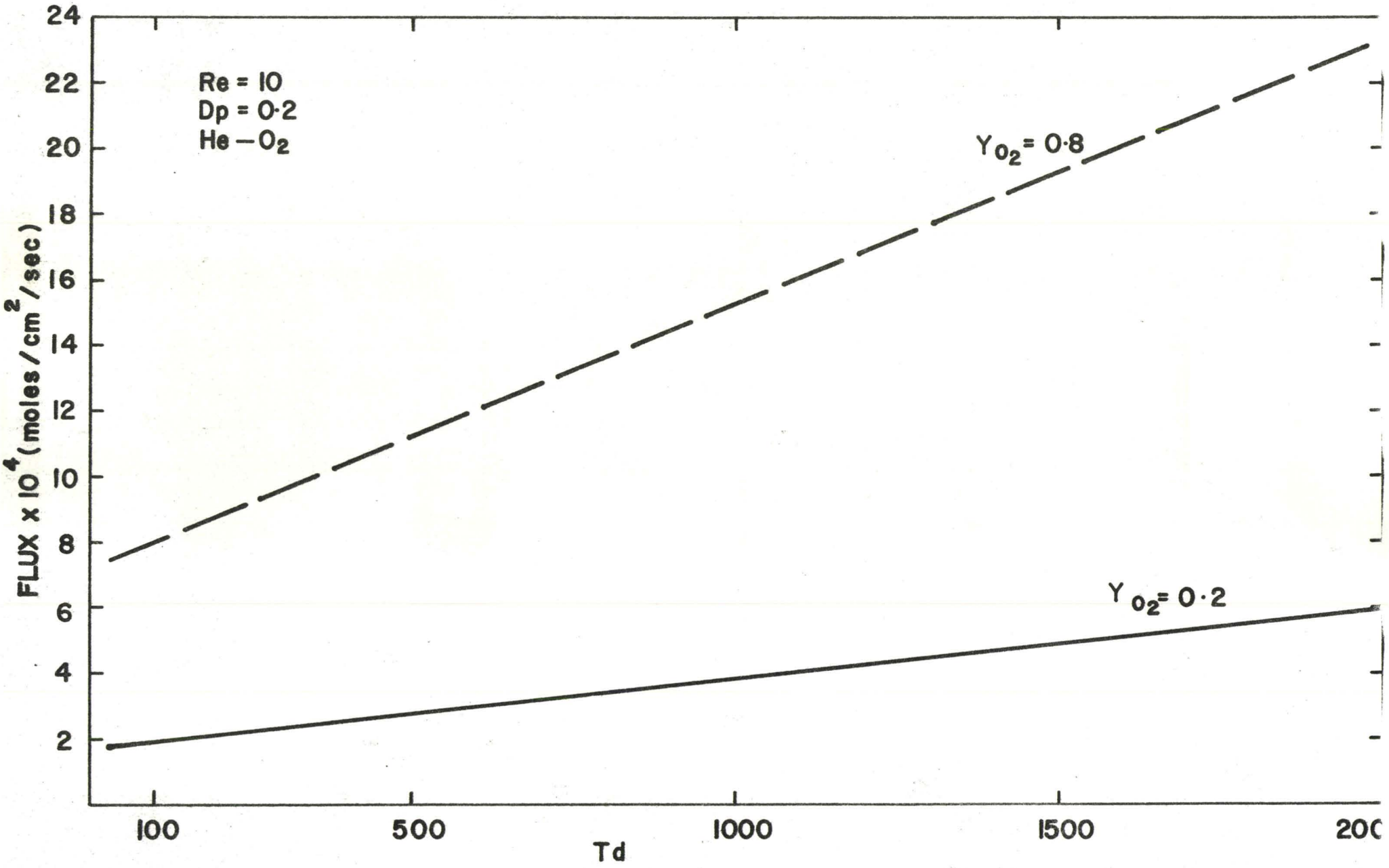

FLUX vs TEMPERATURE FIG.(R–2D)

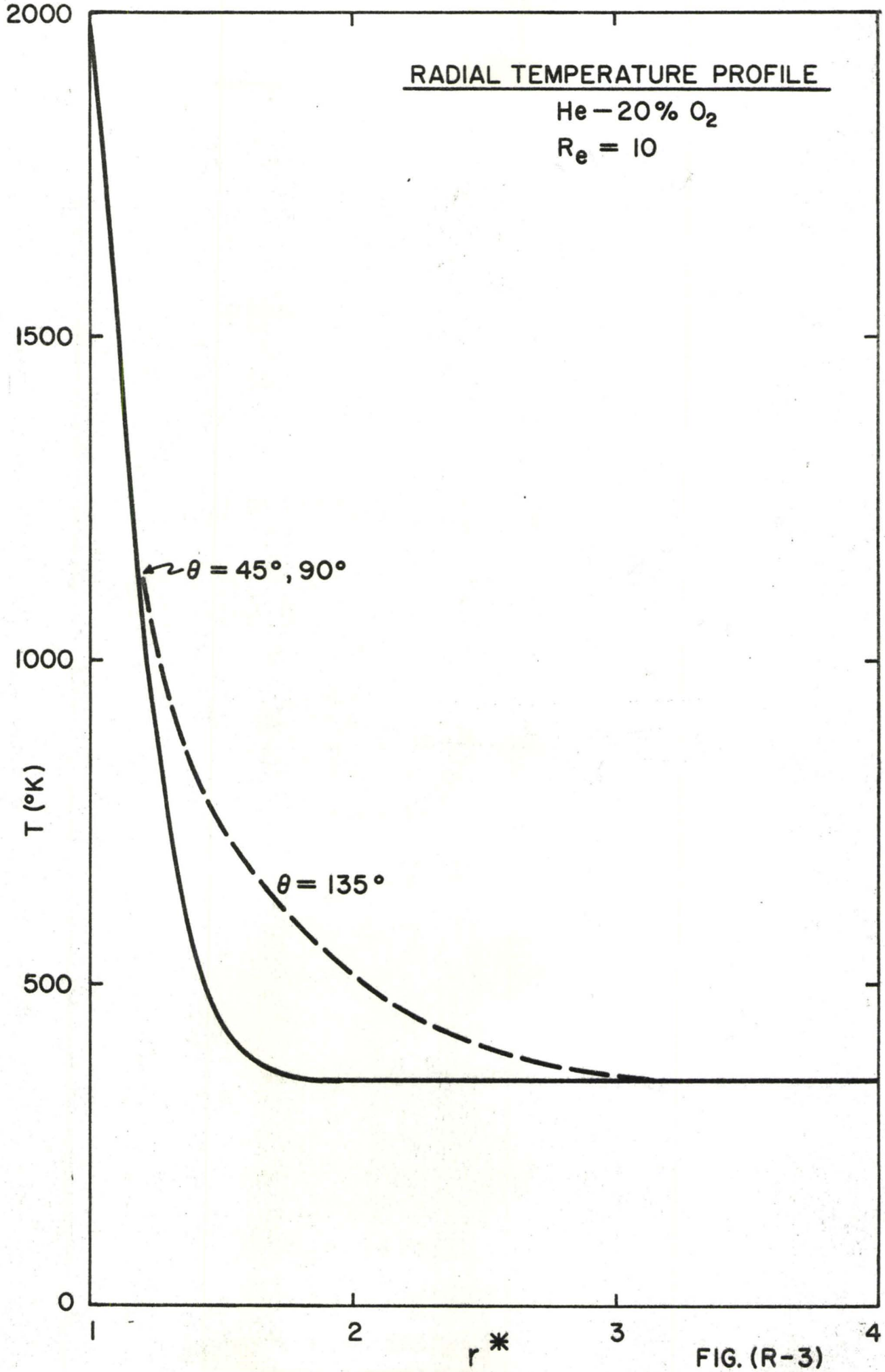
RADIAL TEMPERATURE PROFILE
He – 20% O_2
R_e = 10
θ = 45°, 90°
θ = 135°
T (°K)
r*
2000
1500
1000
500
0
1
2
3
4

FIG. (R-3)

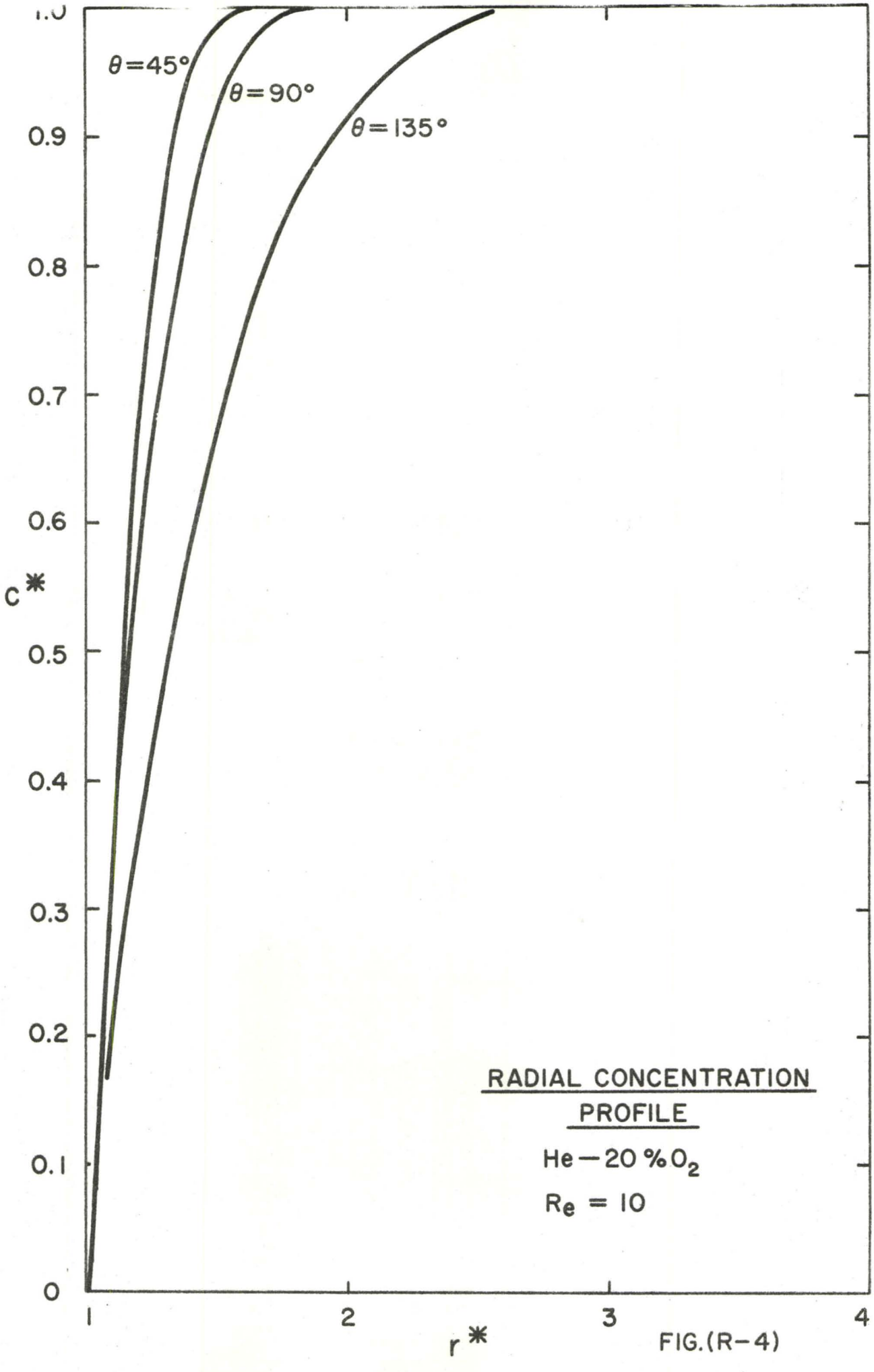
θ=45°
θ=90°
θ=135°
1.0
0.9
0.8
0.7
0.6
0.5
0.4
0.3
0.2
0.1
0
c*
1
2
3
4
r*
RADIAL CONCENTRATION PROFILE
He — 20 % O2
Re = 10

FIG.(R-4)

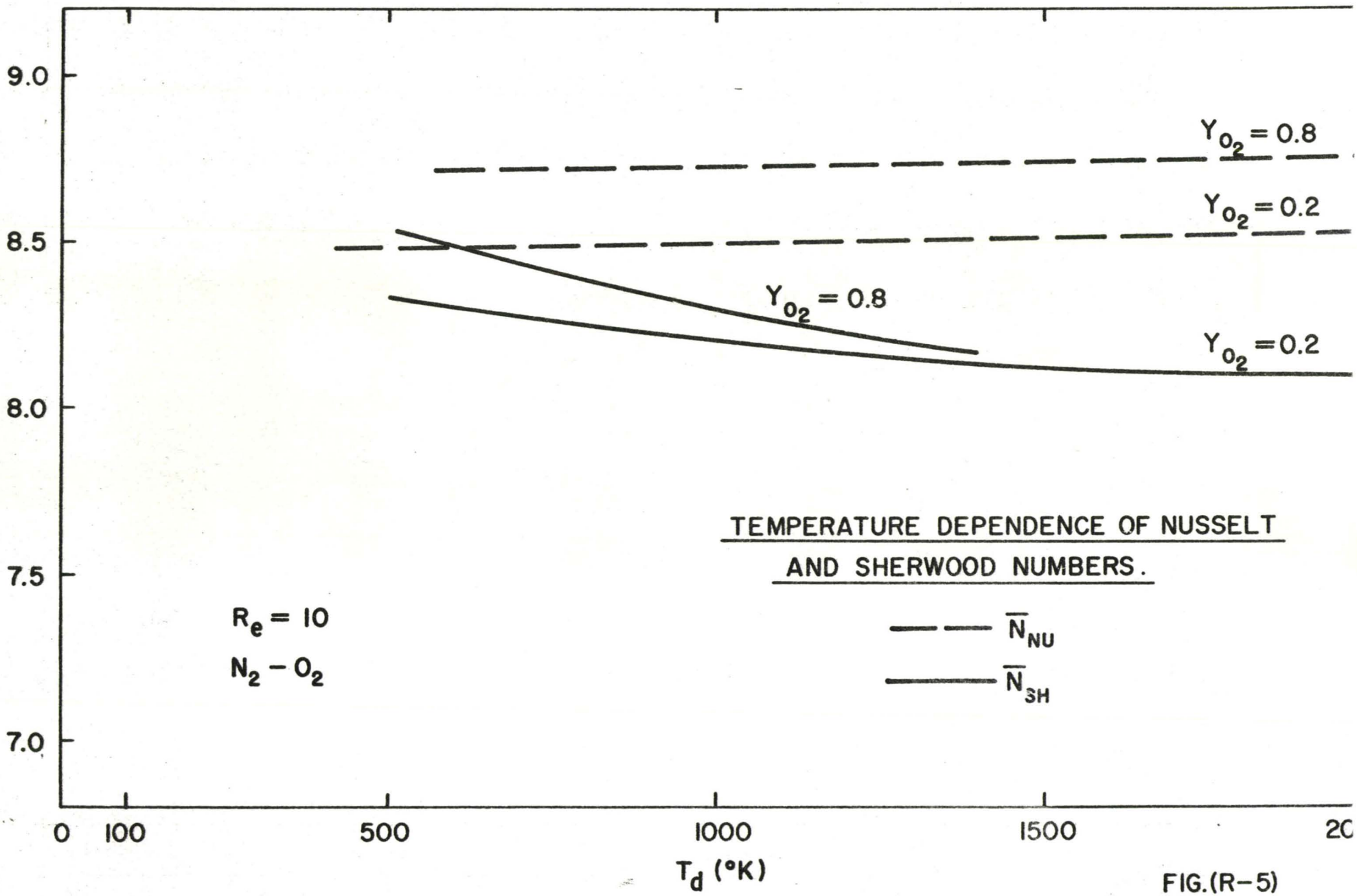

TEMPERATURE DEPENDENCE OF NUSSELT AND SHERWOOD NUMBERS.

FIG.(R-5)

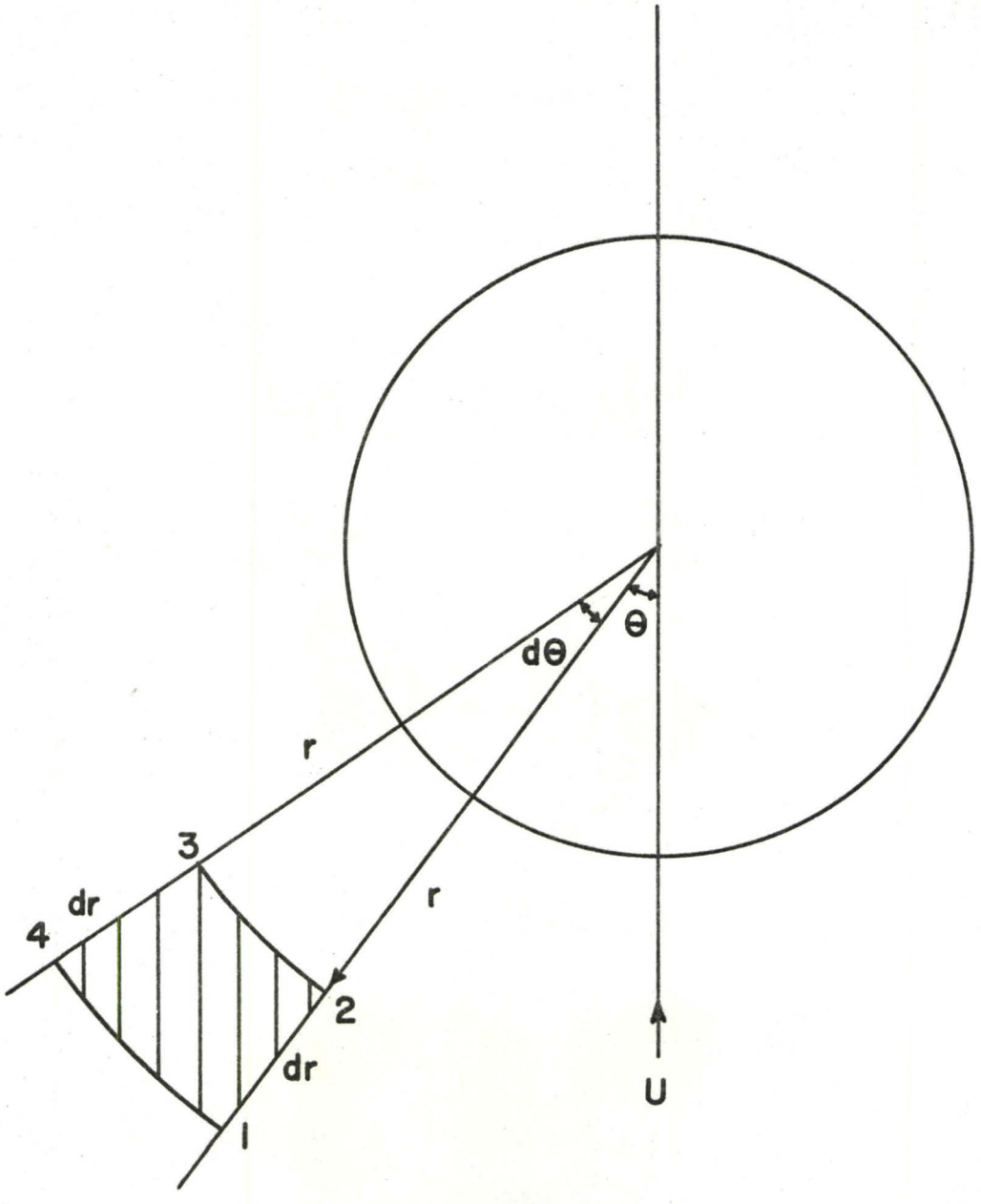

BASIC VOLUME ELEMENT — CONVECTION EQUATION

FIG. (A–1)